Novel Cycles Using Carbon Dioxide as Working Fluid

New Ways to Utilize Energy from Low-Grade Heat Sources

Licentiate Thesis
by
Yang Chen

Stockholm, May 2006

School of Industrial Engineering and Management
Department of Energy Technology
Division of Applied Thermodynamics and Refrigeration

Novel Cycles Using Carbon Dioxide as Working fluid
New Ways to Utilize Energy from Low-Grade Heat Sources
Yang Chen

Trita REFR Report No. 06/50
ISSN 1102-0245
ISRN KTH/REFR/R-06/50-SE
ISBN 91-7178-410-1

Licentiate Thesis by Yang Chen
School of Industrial Engineering and Management
Department of Energy Technology
Division of Applied Thermodynamics and Refrigeration

Printed by Universitetsservice US AB
Stockholm, 2006

Abstract

Energy consumption for heating and air conditioning (A/C) is increasing dramatically. In the EU, over 40% of primary energy consumption is used for heating or cooling in buildings, for domestic hot water supply, for industrial process heat and for heat in the service sector. The majority of this energy is currently produced from imported and polluting fossil fuels or from electricity largely generated by fossil fuels or nuclear power (according to the research done by EUFORES[1]).

Coal, oil and gas, which are called fossil fuels, provide around 66% of the world's electrical power, and meets 95% of the world's total energy demand (including heating, transport, electricity generation and other uses). With the increasing consumption of fossil fuels, more and more environmental problems, such as global warming, ozone depletion and atmospheric pollution, have arisen. Furthermore, with the fast development of industry, energy shortages and blackouts have appeared more and more frequently all over the world.

Due to the reasons mentioned above, utilizing a low-grade heat source for energy production has attracted more and more attention for its potential in reducing fossil fuel consumptions as well as environmental pollution.

Many ongoing research projects in the low-grade heat source utilization area are based on so-called organic Rankine cycles (ORCs) and Kalina cycles (binary fluids and fluid mixtures). However, the drawbacks of these cycles are numerous: for ORC, the working fluids such as R113 and R123 are expensive and strong climate-changing gases themselves. Furthermore, the phase changing of organic working fluid during the heating process creates so-called “pinching” in the heat exchanger and

1 European Forum for Renewable Energy Sources

thus limits heat exchanger performance. For Kalina cycles, the heat transfer characteristics of the fluid mixtures are always poorer than the pure working fluid. Moreover, ammonia, which is the most commonly used working fluid in the Kalina cycle, is highly toxic and corrosive (Yan, 1991, Thorin, 2000)

Compared with these working fluids, carbon dioxide (CO_2) as an environmentally benign natural working fluid has many advantages. It is inexpensive, non-explosive, non-flammable and abundant in the nature. In addition, it has no ozone depleting potential (ODP) and low global warming potential (GWP). As a pure working fluid, it also has better heat transfer characteristics than fluid mixtures. Moreover, due to its relatively high working pressure, the carbon dioxide system is more compact than the system operating with other working fluids.

Due to the character of carbon dioxide's critical point (7.38 Mpa/1070.38psi, 31.1°C/87.98°F), the carbon dioxide power cycle will work as a transcritical cycle or a Brayton cycle. The main difference between these two types of cycles is whether the cycle is partially located in the supercritical region or totally located in the supercritical region.

This licentiate thesis proposes and analyzes three carbon dioxide novel cycles, namely: the carbon dioxide transcritical power cycle, the carbon dioxide Brayton cycle and the carbon dioxide cooling and power combined cycle. Due to the different characteristics of each cycle, the three cycles are suitable for different applications. The CO_2 transcritical power cycle is suitable for harvesting energy from low-grade heat sources, near which a low temperature heat sink is accessible. The CO_2 Brayton cycle is suitable for harvesting the energy from relatively high-grade heat sources when there is no low temperature heat sink available. The CO_2 cooling and power combined cycle is suitable for applications, where both power and cooling are needed (e.g. automobile applications, in which

the cycle can utilize the energy in the engine exhaust gasses to produce power and provide cooling/heating to the mobile compartment room at the same time).

Several models have been developed using the software known as Engineering Equation Solver (EES)[2] for both cycle analysis and computer aided heat exchanger design. Different cycle working conditions have been simulated and different working parameters' influence on the cycle performance has been explained. In addition, Refprop 7.0[3] is used for calculating the working fluid properties and the CFD tool Femlab has been employed to investigate the particular phenomena influencing the heat exchanger performance.

2 Engineering Equation Solver: http://www.fchart.com/ees/ees.shtml

3 Refprop 7.0: http://www.nist.gov/srd/nist23.htm

Preface

This thesis is based on the following papers, which are enclosed at the end.

I. Y. Chen, P. Lundqvist, P. Platell
"Theoretical Research of Carbon Dioxide Power Cycle Application in Automobile Industry to Reduce Vehicle's Fuel Consumption"
Paper published in Applied Thermal Engineering 25 (2005), pp 2041–2053

II. Y. Chen, P. Lundqvist, A. Johansson, P. Platell
"A comparative study of the Carbon Dioxide Transcritical Power Cycle compared with an Organic Rankine Cycle with R123 as working fluid in Waste Heat Recovery"
Paper accepted for publication by Applied Thermal Engineering, 2006

III. Y. Chen, P. Lundqvist
"Carbon dioxide cooling and power combined cycle for mobile applications".
Paper published and presented at 7th IIR Gustav Lorentzen Conference on Natural Working Fluids, Trondheim, Norway, May 28-31, 2006

IV. Y. Chen
"Carbon Dioxide Transcritical Power Cycle Discussion"
Trita REFR Report 2005, No. 05/49, ISSN 1102-0245, ISRN KTH/REFR/R-05/49-SE.

Acknowledgements

After two years of PhD studies at the Division of Applied Thermodynamics and Refrigeration, Energy Department, Royal Institute of Technology, I can finally submit this thesis. Although it may not be perfect, I hope it is a complete summary of my two years of study.

During these two years of study, there are so many people I should gratitude:

First of all, I want to take this chance to express my sincere gratitude to my supervisor, Professor Per Lundqvist for his always wisely guidance, his constant humor and his continual patience through these two years of study. All in all, thanks for being such a good supervisor! Without him, this thesis would not be possible.

Thanks to Peter Platell, his father Ove Platell and all the other industry partners for introducing me to the interesting R&D world and for all the help you offered.

Special thanks go to Professor Björn Palm for his support and help throughout my studies. His hard working is always a good example and inspiring to me.

I am also very grateful to Professor Emeritus Eric Granryd and Dr. Anders Johansson for valuable comments on my thesis and to Dorothy Furberg for correcting my English.

I would like to thank to the entire faculty at the Department of Energy Technology and all the PhD students at the Division of Applied Thermodynamics and Refrigeration (especially, Dr. Nabil Kassem , Dr. Hans Jonsson, Åke Melinder, Inga Du Rietz, Susy Mathew, Dr. Jaime Arias, Dr. Joachim Claesson, Dr.

Rahmatollah Khodabandeh, Guest Prof. Timothy Ameel, Peter Hill, Jan Erik Nowacki, Benny Andersson, Benny Sjöberg, Wimolsiri Pridasawas, Getachew Bekele, Primal Fernando, Claudi Martin, Wahib Owhaib, Oxana Samoteeva, Samer Sawalha, Raul Anton, Richard Furberg, Cecilia Hägg, Shota Nozadze, Branko Simanic, Paulina Bohdanowicz, Manish Ranjan) for being such good colleagues. I feel really lucky that I can study here with all of them.

Moreover, I should thank all my relatives, friends and especially Lei, for their support and encouragements.

Last but not least, I want to express my gratitude to my parents, Xiaoming Tian and Jiabao Chen, and to my grandparents, Suxun Yan and Zairen Tian for their love, support and constant care.

Table of Contents

List of Tables

List of Figures

Nomenclature

Roman		
A	Area	m^2
b	Average length of the heat exchanger pipes	m
CO_2	Carbon dioxide	-
Cp	Specific heat	kJ/kg·k
COP	Coefficient of performance	-
d_h	Hydraulic diameter	m
f	Friction factor	-
GWP	Global warming potential	-
h	Convection heat transfer coefficient	kJ/kg·k
IHX	Internal heat exchanger	-
k	Thermal conductivity of the fluid	W/m·k
L_c	Characteristic length	m
L	Length in air flow direction	m
$\dot{m}$	Mass flow	kg/s
Nu	Nusselt number	-
ODP	Ozone deleting potential	-
ORC	Organic Rankine cycle	-
p	Wet perimeter	m
p	Pressure inside the tube	bar
Pr	Prandtl number	-
Q	Power of heat exchanger (transferred heat)	kW
Re	Reynolds number	-
R	Heat exchanger tube radius	degree

s	Distance between every two plates	m
t	Tube wall thickness	m
u	Velocity	m/s
Δt	Temperature change	°C
Δp	Pressure drop	bar
ν	Kinematics viscosity of fluid	M^2/s
μ	Dynamic viscosity of fluid	Pa·s
ρ	Density	kg/m^3
σ_1	Hoop stress	MPa
η	Cycle thermal efficiency	-
Subscript		
o	Outside	
c	Compressor outlet	
e	Expansion inlet	
in	Heat source inlet	
out	Heat source outlet	
eff.	Efficiency	
area	Surface area	
cross	Heat exchanger cross section area	M^2
infinite	Heat exchanger air inlet	
local	Symbol for local value	
wall	Heat exchanger surface	
a-k	Points of cycle working route	

1 Introduction

1.1 Motivation

Due to rapid development all over the world, the energy usage is increasing everywhere. According to the research carried out by the International Energy Agency (IEA) in 2002, the world's energy demand is expected to increase by about 1.7% per annum until the year 2030. Among the energy sources, fossil fuels dominate about 80% of the total energy supply, while renewable energy only contributes with 11% nowadays (IEA report, 2004). Due to the large consumption of fossil fuels, more and more environmental problems such as global warming, ozone depletion and air pollution etc., have been caused. Furthermore, along with continually increasing energy demand, energy shortages and blackouts have appeared more and more frequently all over the world. For these reasons, increasing energy usage efficiency by recovering the energy from low-grade heat sources for power production has received an increasing interest.

When utilizing the energy in most low-grade heat sources, the heat source temperature will not show a constant temperature during the process, but rather a gliding temperature instead. This is mainly due to two reasons: either the temperature level of the heat source is not high enough or the amount of the heat source is limited (i.e. the mass flow of the heat source is limited), thus the heat source flow's temperature starts to drop as soon as the energy in it is being used. Consequently, the traditional steam Rankine cycle does not give a satisfying performance due to its low thermal efficiency and large volume flows. Furthermore, if the low-grade heat source is not capable

of superheating the working fluid to a certain high temperature, the exhaust gases will have high moisture contents after expansion, which will cause erosion of turbine blades and may also destroy them. As a result, the so-called organic Rankine cycle (ORC) and Kalina cycle (binary fluids and fluid mixtures) are proposed for their potential in utilizing the energy in low-grade waste heat.

The organic Rankine cycle (ORC) is a non-superheating thermodynamic cycle that uses an organic working fluid (such as R113 and R123) to generate power (electricity). The working fluid is heated to saturated vapor and the expanding vapor is used to drive an expansion machine. The main advantage of ORC is that for many organic compounds, it is not necessary to superheat the working fluid to avoid moisture erosion at the turbine outlet, which may result in higher cycle efficiency. For the Kalina cycle, the advantage is that the zeotropic fluid mixtures can better match the heat source temperature, so that better efficiency can be expected. However, the drawbacks of these cycles are also numerous: for ORC, the working fluids such as R113 and R123 are expensive, strong climate-changing gases themselves and also ozone depleting. In addition, the phase-changing of organic compounds during the heating process (evaporation) may introduce so-called "pinching" in the heat exchanger, which produces irreversibilities and counteracts the effort to improve the cycle efficiency from a thermodynamic viewpoint. For Kalina cycles, using fluid mixtures will yield a poorer heat transfer performance than using pure working fluid. Moreover, ammonia, which is the most commonly used working fluid in the Kalina cycle, is highly toxic and corrosive.

Compared to the working fluids that have been mentioned, carbon dioxide shows more potential in utilizing the energy in low-grade heat sources. This is mainly due to the character of carbon dioxide's temperature profile in the supercritical region that can provide a better match to the heat source temperature

glide than the other working fluids mentioned above (Figure 1-1). Thus the so-called "pinching", which commonly occurs for other working fluids, will not be encountered inside the CO_2 counter flow heat exchanger.

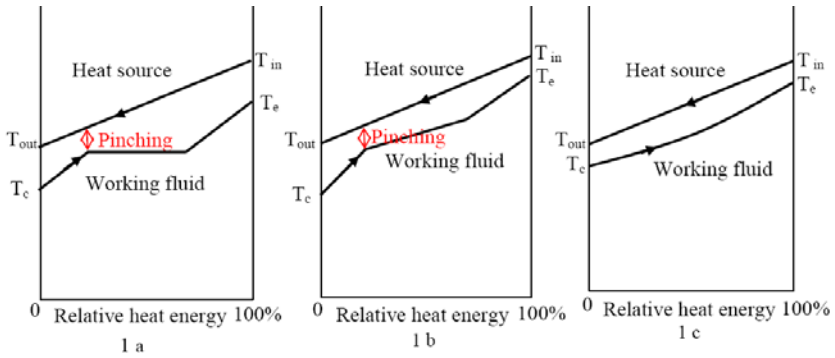

Figure 1-1 Schematic representation chart of the heat transfer between the low-grade heat source and working fluid in the main heat exchanger: (1a) pure fluid; (1b) zeotropic fluid mixtures; (1c) carbon dioxide

The reason why the match between the heat source temperature profile and the working fluid temperature profile is so important when utilizing the energy in low-grade heat sources can be explained by a simple example. A "typical" cycle (Carnot cycle) with a varying heat source temperature and a constant heat sink temperature of 293 K is employed for this example, which is schematically showed in Figure 1-2

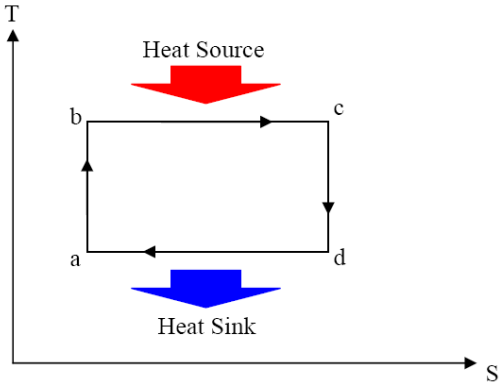

Figure 1-2 Schematic illustration of a typical cycle— Carnot cycle

As show in Figure 1-2, the "typical" cycle consists of following processes:

- a to b: Isentropic compression
- b to c: Isothermal heat supply
- c to d: Isentropic expansion
- d to a: Isothermal heat rejection

And the thermal efficiency of the cycle will be:

$$\eta = \frac{W_{output}}{Q_{input}} = 1 - \frac{T_{da}}{T_{bc}} \qquad \text{Equation 1-1}$$

But since $T_{bc} = T_{source} - \Delta T$ and $T_{da} = T_{sink} + \Delta T$ we get:

$$\eta = 1 - \frac{T_{\sin k} + \Delta T}{T_{source} - \Delta T} \qquad \text{Equation 1-2}$$

The calculated cycle efficiency is illustrated in Figure 1-3, from which one can see that the cycle with the smaller temperature differences, ΔT, in the heat exchangers will achieve a higher efficiency. Furthermore, the temperature difference plays a more important role at low heat source temperatures than at high heat source temperatures. For example, at a heat source temperature of 360 K, the cycle with ΔT = 10 K in both heat exchangers achieves almost two times higher efficiency than the cycle with ΔT = 20 K. While at 440 K heat source temperature, the cycle with ΔT = 10 K in both heat exchangers only achieves an efficiency of 1.2 times that of the cycle with ΔT = 20 K. Therefore, the better heat source matching characteristics of CO_2 makes this cycle more interesting for the utilization of energy in low-grade heat sources.

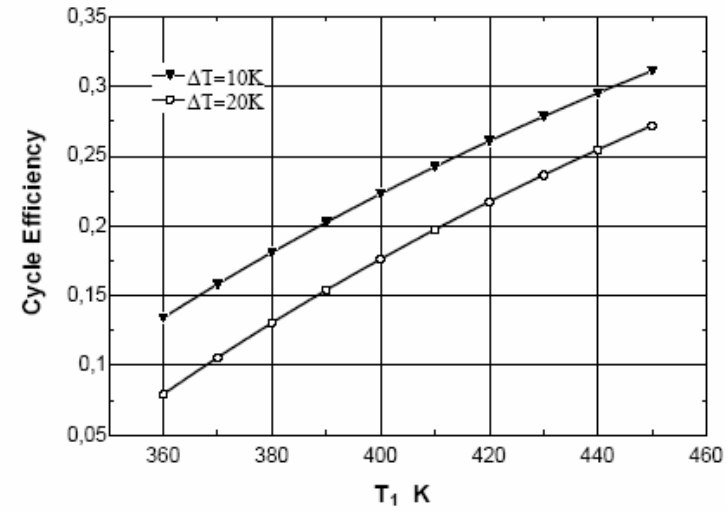

Figure 1-3 Cycle efficiency with varying heat source temperatures and a constant heat sink temperature (293 K) for different temperature differences in the two heat exchangers (gas heater and condenser)

All the discussions above show that there is a great potential for energy saving by utilizing the energy in low-grade heat sources and CO_2 has many advantages as a working fluid for the conversion of energy from a low-grade heat source into useful energy. This thesis work was proposed for these reasons.

1.2 Thesis Contribution

This thesis contributes to the knowledge base by analyzing the potential of different CO_2 novel cycles and corresponding systems. Several CO_2 system layouts and applications are suggested, and different factors that influence the cycle performance are analyzed. A new CO_2 cooling and power combined cycle is proposed and studied for its performance, working conditions optimization, etc. In addition, a number of models were run though in Engineering Equation Solver (EES) for both cycle analysis and computer aided heat exchanger design. Different cycle working conditions have been simulated and different working parameters' influences on the cycle performance have been analyzed. Moreover, several modules

have also been built in the CFD tool Femlab in order to show the influence of thermal conduction inside the heat exchanger material on the heat exchanger performance.

2 Background

2.1 Working Fluid Comparison

Table 2-1 gives the properties of various working fluids proposed in the literature.

There are several factors that have to be considered when selecting the working fluid for the proposed cycles. If one considers the toxicity and flammability, the working fluid with ASHRAE level A1 should be the safest one to use. Therefore, working fluids like ammonia and isobutene are disregarded. If one considers the environmental impact, the working fluid with the lowest ozone depleting potential (ODP) and global warming potential (GWP) should be selected. Therefore, working fluids like sulfur hexafluoride and perflupropane are neglected. Furthermore, if one considers the heat transfer performance, fluid mixtures often show poorer heat transfer performance than pure working fluids. Fluid mixtures are therefore less desirable from this viewpoint. After taking all these into account, carbon dioxide proved to be the most promising working fluid to be selected.

Carbon dioxide has many advantages as a working fluid for the proposed system: it is an environmentally benign natural working fluid and very safe to use. It is abundant in nature and comes at low cost. Moreover, the chemical thermodynamic properties of carbon dioxide have been thoroughly studied and there is therefore sufficient knowledge about them.

Table 2-1 Properties of different fluids

Fluid name	ASHRAE No.	Formula	Critical temp. (°C)	Critical press. (Bar)	ASHRAE Level for safety[6]	ODP rel. R11	GWP rel. CO_2
Carbon dioxide	R744	CO_2	30.98	73.8	A1	0	1
Water	R718	H_2O	373.89	22.10	A1	0	-
Hydroflorocarbon	R134a	CH_2FCF_3	101.1	40.7	A1	0	1300
Butane	R600	C_4H_{10}	152	37.9	A3	0	0
Isobutane	R600a	C_4H_{10}	134.7	36.4	A3	0	<20
Sulfur Dioxide	R764	SO_2	157.5	78.8	B1	0	-
Ammonia	R717	NH_3	132.89	112.8	B2	0	<1
Sulfur Hexafluoride	R-7146	SF_6	45.56	37.6	?	?	239000
Perfluoropropane	R218	C_3F_8	71.89	26.8	?	0	7000
Zeotropic mixture	R407C	R32/R125/R134a (23/25/52)	87.3	48.2	A1	0	1600
Azeotropic mixture	R500	R12 / R152a (73.8%26.2%)	102.1	41.7	A1	0.605	7870

6 In ANSI/ASHRAE Standard 15-1992, refrigerants are classified according to the hazard involved in their use. Group A1 refrigerant are the least hazardous, Group B3 the most hazardous. Details can be found in Appendix 1

Compared to other working fluids listed in Table 2-1, carbon dioxide has a unique characteristic in its critical point, i.e. high critical pressure but low critical temperature (7.38 Mpa/1070.38psi and 31.1°C/87.98°F). Thanks to this characteristic, carbon dioxide has many advantages in utilizing the energy from low-grade heat sources: the high pressure makes the CO_2 system more compact compared with systems using other working fluids. The energy in the expansion outlet carbon dioxide can be recovered within the cycle through regenerative heat exchanger (i.e. a regenerator), thus the high working pressure is helpful in reducing the regenerator size and excellent heat transfer characteristics helps to minimize the influence of pressure drop on the cycle efficiency. Furthermore, the low critical temperature means even a low temperature heat source can give a trans-critical cycle with the "gliding" temperature profile that provides a better match to the heat source temperature glide in comparison with other working fluids (as mentioned in the Introduction). Moreover, since the heating process takes place in the supercritical region, some complexity involved in a phase changing process (e.g. flow maldistribution) can be avoided.

2.2 History of CO_2 Power Cycle

Research on the CO_2 power cycle was first proposed by Sulzer Bros in 1948 and later several countries, such as the Soviet Union, Italy and the United States, got involved in the research on such a cycle. After its prosperity in the 1960s, research on the cycle, however, dwindled for many years until the 1990s, mainly due to limited amount of suitable (e.g. nuclear) heat sources and limited knowledge in suitable compact heat exchangers and suitable expansion machines (Dostal, 2004). After the 1990s and development of compact heat exchangers and materials, etc., renewed interest was shown in the carbon dioxide power cycle and much research has been carried out (Dostal, 2004; Chang, 2002). Nevertheless, most investigations have focused on a carbon dioxide power cycle with a nuclear

reactor as a heat source, thus the cycle working with a high-grade heat source (up to 800 °C) and high pressures in both the gas heater and gas cooler (CO_2 Brayton cycle). Research on employing such a cycle for low-grade heat source recovery has been relatively limited.

2.3 System Illustration and Corresponding Cycle Description

There are two systems proposed in this thesis: the carbon dioxide bottoming system and the carbon dioxide cooling and power combined system.

2.3.1 The CO_2 bottoming system and corresponding cycles

The CO_2 bottoming system consists of four main parts, namely: a gas heater, turbine, condenser (gas cooler) and pump (Figure 2-1). In this system, the carbon dioxide is first pumped to a supercritical pressure, and then heated in the gas heater. The heated supercritical carbon dioxide will expand in the turbine. The vapor discharged from the turbine outlet will then be cooled and condensed in a condenser (gas cooler). The internal heat exchanger (regenerator) is added to the basic system to optimize the system performance. The importance of utilizing a regenerator in a carbon dioxide transcritical power cycle will be shown latter part of this thesis.

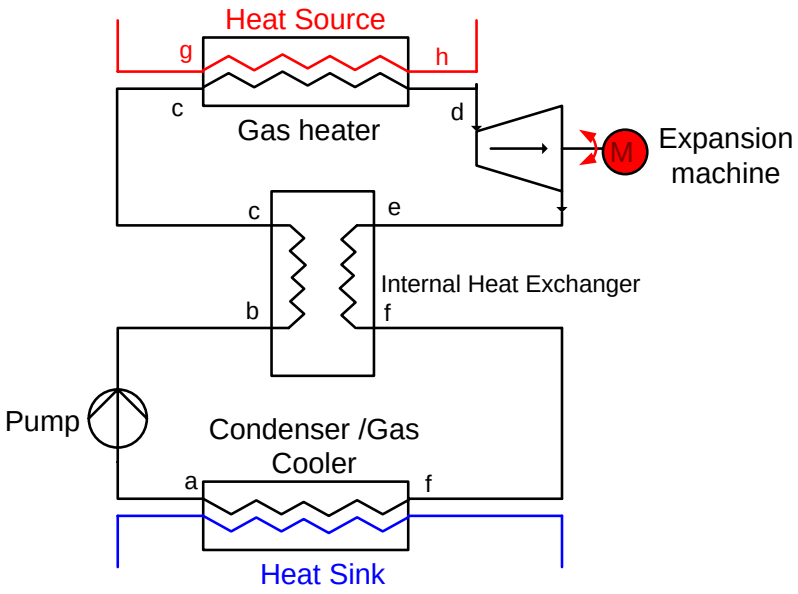

Figure 2-1 Schematic of the carbon dioxide power system (for both Brayton cycle and transcritical cycle)

The corresponding cycles of this system are the carbon dioxide transcritical power cycle and the carbon dioxide Brayton cycle respectively. Both cycles consist of four processes, namely: compression (a-b), isobaric heat supply (b-d), expansion (d-e), isobaric heat rejection (e-a). The only difference between these two cycles is whether there is a part of the cycle located in the sub-critical region or not, therefore both cycles are sometimes related to supercritical cycles in the literature. Both cycles are illustrated in the T-S charts as follows (Figure 2-2 & Figure 2-3).

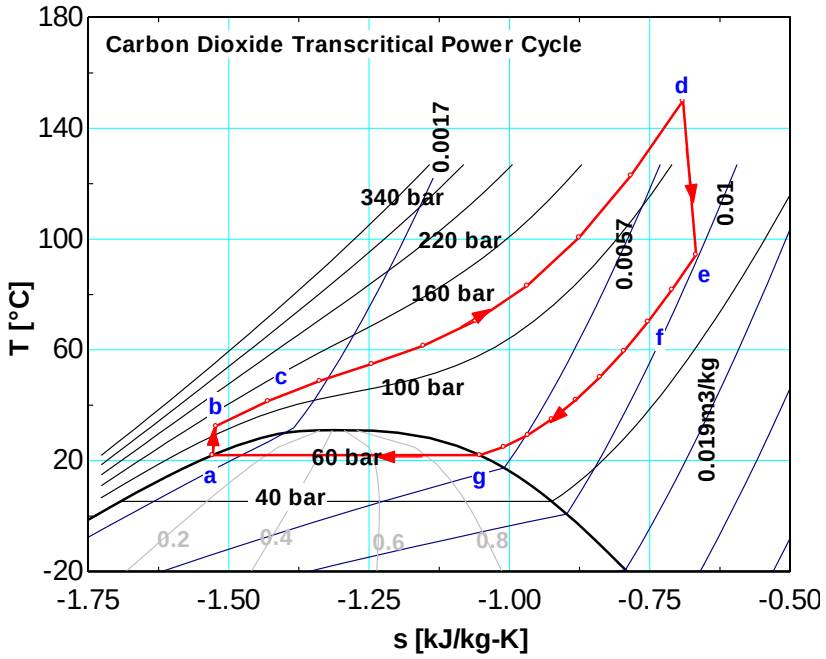

Figure 2-2 Carbon dioxide transcritical cycle T-S chart

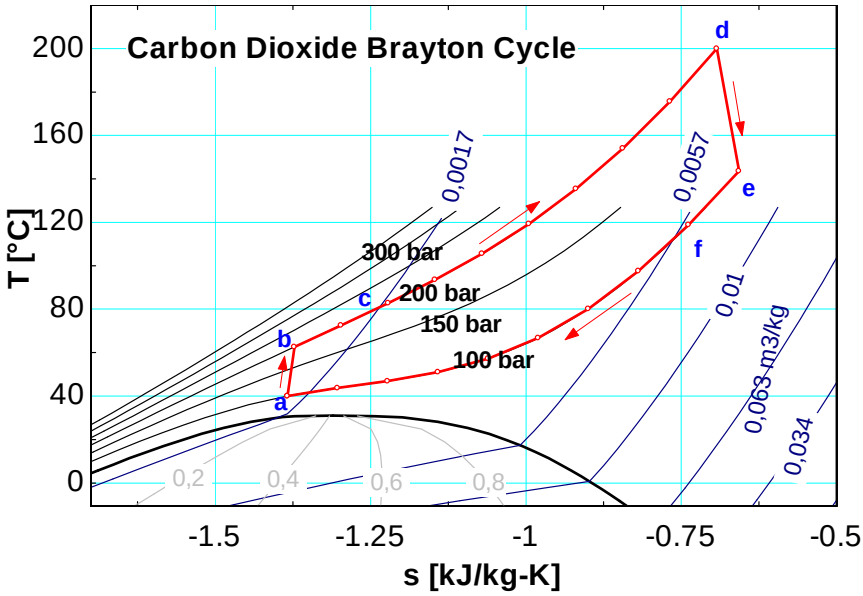

Figure 2-3 Carbon dioxide Brayton cycle T-S chart

2.3.2 The combined system and the corresponding cycle

The carbon dioxide cooling and power combined system is mainly composed of six parts, namely: an evaporator, compressor, gas heater, expander, gas cooler and throttling valve. The system layout and the corresponding cycle's T-S chart are shown respectively as follows (Figure 2-4 & Figure 2-5)

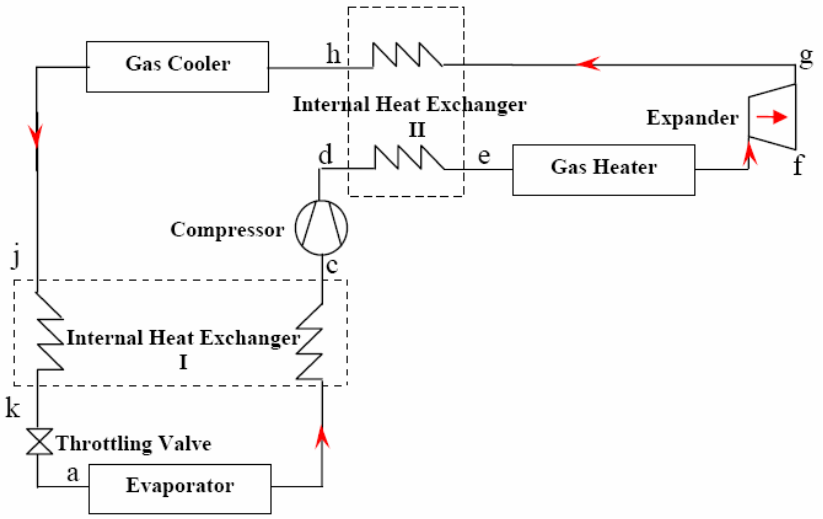

Figure 2-4 Carbon dioxide cooling and power combined system schematic layout

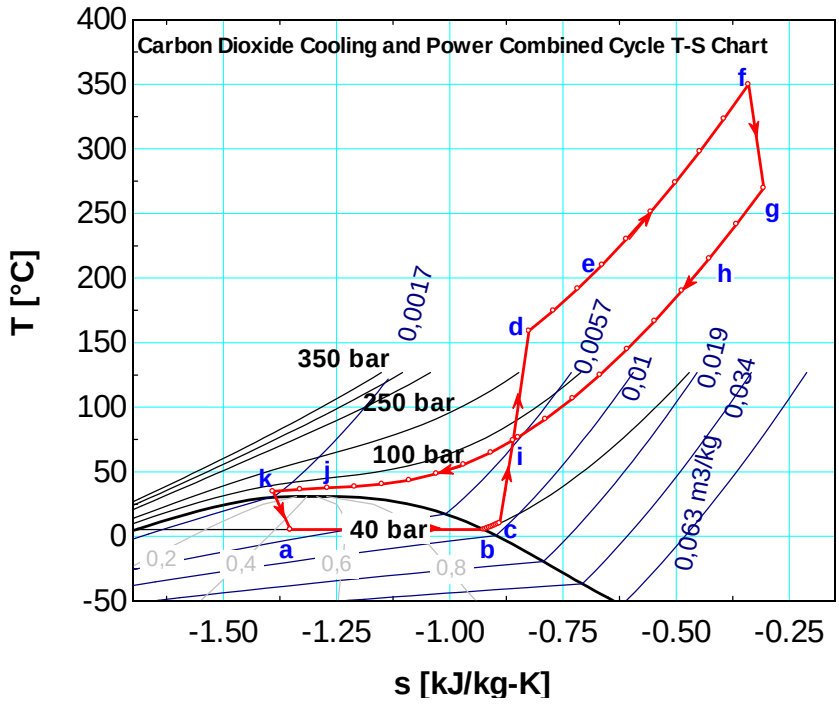

Figure 2-5 Carbon dioxide cooling and power combined cycle T-S chart

The corresponding cycle consists of six processes, namely: compression (c-d), isobaric heat supply (d-f), expansion (f-g), isobaric heat rejection (g-k), throttling (k-a), isobaric heat apply (a-c).

After absorbing heat in the evaporator (a-b), the carbon dioxide will be further heated in the internal heat exchanger I (IHX I) until it becomes slightly superheated (b-c). The superheated carbon dioxide vapor will then be compressed by a compressor to a supercritical pressure (c-d), where supercritical carbon dioxide absorbs the heat first from the expansion outlet carbon dioxide in IHX II (d-e) and then from the heat source in a gas heater (e-f). After that, the supercritical carbon dioxide will be expanded in an expander (f-g) and then cooled by IHX II (g-h), a gas cooler (h-j) and IHX I (j-k) in turn. Finally, it flows though a throttling valve and enters the evaporator (k-a). In the power

part of the combined cycle (d-f-g-i), carbon dioxide will absorb the heat from the low-grade heat source and convert it into useful mechanical work.

The combined cycle is designed to be employed in automobile applications, for which the power part of the combined cycle will utilize the energy in the engine exhaust gases to produce power for the cooling part's compressor.

Traditionally, the COP of a vapour compression refrigeration system is defined as Equation 2-1.

$$COP = \frac{Q_{cooling}}{W} \qquad \textbf{Equation 2-1}$$

Where, $Q_{cooling}$ is the cooling capacity of the cooling system, W is the required compression work of the compressor.

Since the power produced by the combined cycle power part is gained from the engine's waste heat, it is produced "free of charge". The combined cycle can achieve the required cooling capacity with less energy demand for the compression work thus saving fuel and lowering emissions. Consequently, the "new COP" of the combined cycle cooling part can be defined by Equation 2-2[5].

$$COP_{new} = \frac{Q_{cooling}}{W_{new}} = \frac{Q_{cooling}}{W_{basic} - W_{output}} \qquad \textbf{Equation 2-2}$$

Where $Q_{cooling}$ is the required cooling capacity, W_{new} is the new compression work after taking away the energy gained by the combined cycle power part, W_{basic} is the original compression

5 This definition is only useful for a comparison with a conventional system where the extra work, Woutput increases the apparent COP. For a truly heat driven system where $W_{basic} = W_{output}$ the definition gives an infinite COP.

work of the cooling cycle, W_{output} is the work output from the combined cycle power part, i.e. the "free" energy gained from the engine exhaust gas.

2.4 Heat Exchanger Description

2.4.1 Description of the heat exchangers

As already stated in the background part, several of the carbon dioxide power system's main components are heat exchangers, including a gas heater, condenser/gas cooler and internal heat exchanger (regenerator).

RANOTOR[6] heat exchangers are designed and adopted in this thesis work. This kind of exchanger is characterized as a counter current heat exchanger with laminar flow at the heat exchanger outside (gas side). The advantages of this type of heat exchanger are: high power density (kW/m^3), low pressure drop and flexible installation, etc. The shape of this type of heat exchanger is sketched in the following figures (Figure 2-6 and Figure 2-7).

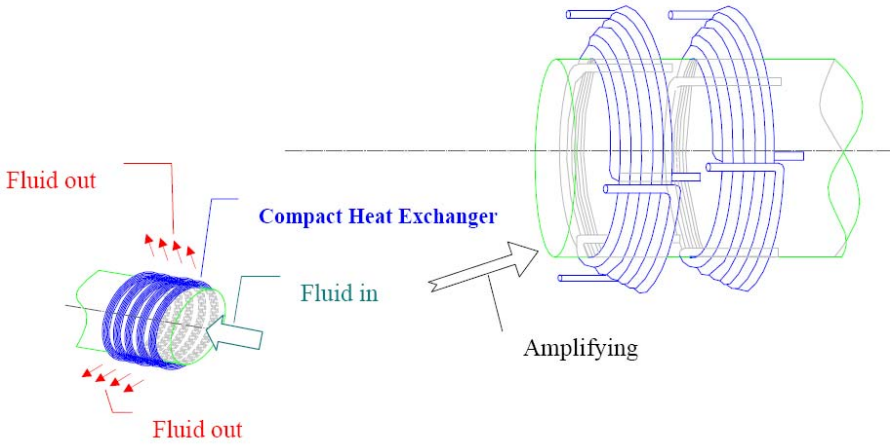

Figure 2-6 RANOTOR heat exchangers

6 Proposed by RANOTOR—A Swedish R&D company

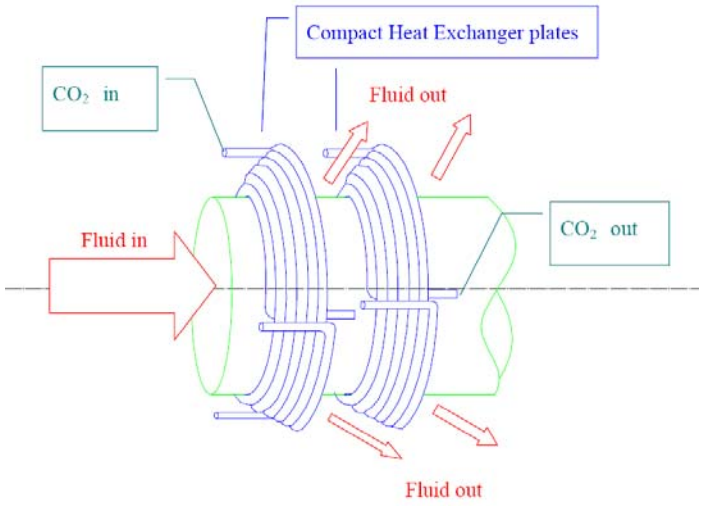

Figure 2-7 RANOTOR heat exchangers

As illustrated in Figures 2-6 and 2-7, this kind of heat exchanger is composed of a number of concentric conical plates, which are made up of several heat exchanger tubes, arranged in parallel. The distance between the heat exchanger plates is 1 mm. For each plate, there are three small diameter (1 mm) tubes placed one after another and bent to the concentric conical shape. Therefore, each heat exchanger plate has three inlets, which are placed on the front side. Carbon dioxide comes from a manifold and goes into the heat exchanger via the three inlets at the same time. After being heated up or cooled down, the exiting carbon dioxide will be collected at the back side of the heat exchanger by the other manifold. The heat source fluid (e.g. exhaust gas, steam, etc.) will flow through the center of the heat exchanger plate and spread out evenly through the aperture between each pair of heat exchanger plates.

2.4.2 Counter flow compact heat exchanger with laminar flow at the airside

According to the surface area density value, the heat exchangers can be divided mainly into three categories:

compact heat exchangers (surface area density above 700 m^2/m^3 on at least one fluid side, which usually has gas flow), laminar flow heat exchangers (surface area density above 3000 m^2/m^3) and micro heat exchangers (surface area density is above about 10000 m^2/m^3). The configurations of a compact heat exchanger are normally plate-fin, tube-fin and prime surface recuperators and compact regenerators. Basic flow arrangements of the two fluids are single-pass cross flow, counter flow and multipass cross-counter flow (R.K. Shah, 1991).

Based on the criteria described above, RANOTOR heat exchangers belong to the category of compact heat exchangers. The flow pattern in the heat exchanger may appear to be cross flow, but it is actually counter flow. This can be explained by the following drawings (Figures 2-8 & 2-9). The left drawing in Figure 2-8 is the top view of one heat exchanger plate, and the one on the right is a schematic illustration to show the angels of the heat exchanger tubes on the heat exchanger plate. As shown in the figure, the heat exchanger plates are designed to have certain angles when bent. Therefore, the heat source fluid flow can be divided into two directions when crossing every small section of the heat exchanger tube (Figure 2-9). Along the X direction, there will be no heat transfer but only fluid flow, while along the Y direction heat transfer will take place. Thus if one integrates along the tube to the total heat exchanger tube length, the heat exchanger will show the heat transfer characteristics of a perfect counter flow heat exchanger. Furthermore, the gas side fluid flow is designed to be laminar flow. Therefore, in general, the RANOTOR heat exchanger is characterized as a counter flow compact heat exchanger with laminar flow at the gas side.

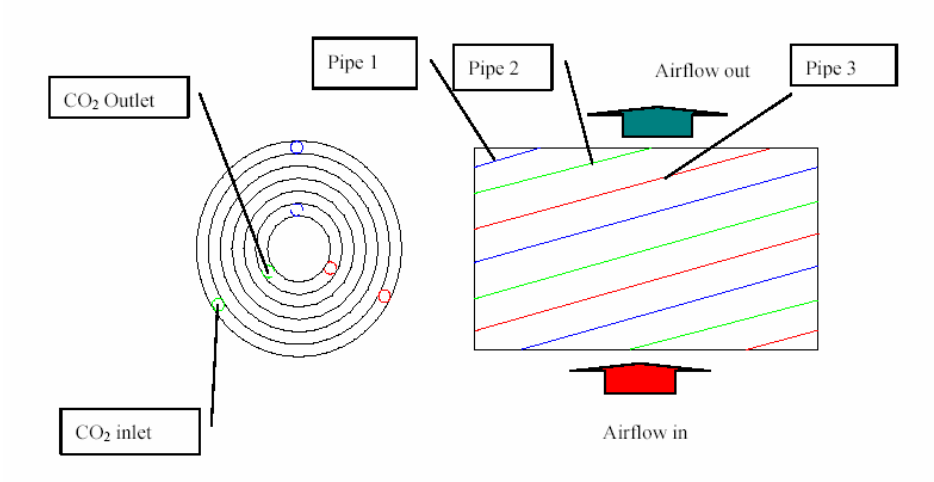

Figure 2-8 Schematic illustration of a RANOTOR compact heat exchanger

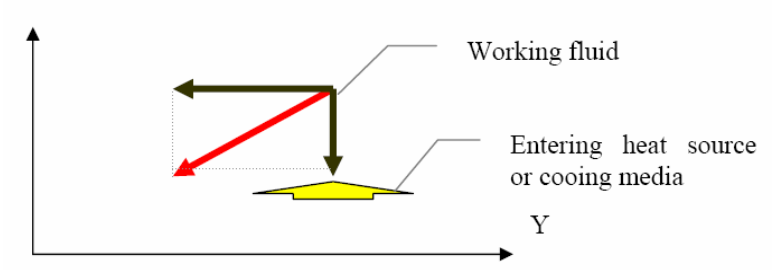

Figure 2-9 Schematic illustration of the flow scheme for a RANOTOR compact heat exchanger

2.4.3 Superiority of laminar flow

Traditionally, turbulent flow is desired in heat exchangers to achieve high heat transfer coefficients. However, for compact heat exchangers, a turbulent flow will require extremely high fan power and normally achieve lower heat transfer than laminar flow. Thus, laminar flow is more desirable for compact heat exchangers due to the fact that it achieves a higher heat transfer coefficient with a smaller heat exchanger volume and lower fan power compared with the turbulent flow. The reason

why laminar flow can achieve a higher heat transfer coefficient in compact heat exchangers can be explained as follows:

The heat transfer coefficient, *h*, can be expressed by Equation 2-3:

$$h = \frac{Nu \times k}{L_c} \qquad \text{Equation 2-3}$$

Where

h — Heat transfer coefficient
Nu — Nusselt number
k — Thermal conductivity
L_c —Hydraulic diameter

For laminar flow, the Nusselt number will be constant for a certain geometry of a heat exchanger and *k* is constant for a certain fluid bulk mean temperature. Thus the smaller the hydraulic diameter is, the higher the heat transfer coefficient will be. Therefore, when the hydraulic diameter is greatly reduced, an extremely high heat transfer coefficient can be expected although the flow is still in the laminar region.

The superiority of laminar flow is clearly illustrated in an example from the book Heat Exchanger Engineering (1991): For water at 310 K using *k* = 0.628 W/m·k and *Pr* = 4.62, *h* is shown as a function of the tube diameter (Figure 2-10). It can be seen that the heat transfer coefficient for a 20 mm diameter tube at $\mathrm{Re} = 10^4$ is the same as a 1 mm diameter tube in laminar flow. *h* is also the same for a 20 mm diameter tube at $\mathrm{Re} = 5 \times 10^4$ and a 0.3 mm diameter tube in laminar flow.

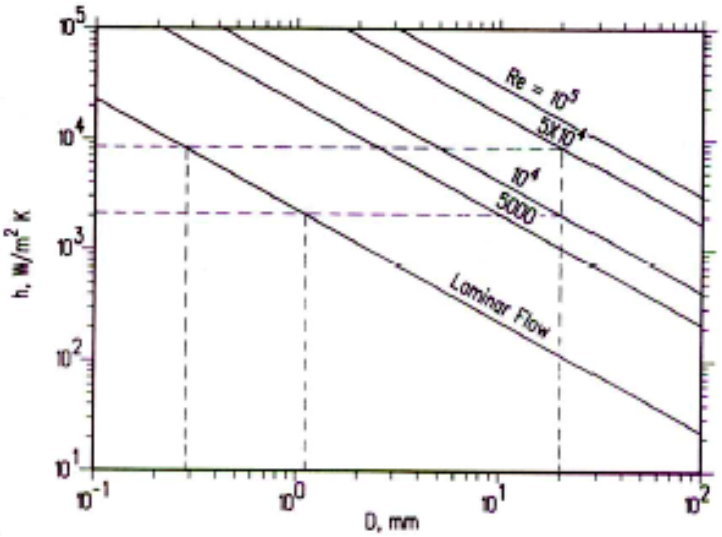

Figure 2-10 *Superiority of laminar flow heat transfer coefficient vs. tube diameter (Shah, 1991)*

3 Objectives and Approach

The main objective of this project is to investigate the potential of the proposed cycles and systems in utilizing the energy from low-grade heat sources in order to provide cooling/heating in a more sustainable way. The research work is performed both by computer aided simulation and experimental investigation.

To achieve the final goal, the work should be performed in several steps: computer aided investigation on the possibility and potential of the proposed cycles in exploiting the energy from a low-grade heat source; a thorough study of the characteristics of the proposed cycle, which includes the properties of the working fluid (CO_2), different working parameters' influences on the cycle performance, and heat transfer performance for the proposed system under different working conditions; designing the appropriate system that can employ the proposed carbon dioxide power cycle; experimental validation of different components performances; experimental investigation of the whole system performance under different operating conditions; and finally experimental investigation of system optimization.

For the current licentiate thesis, the objective is to verify the proposed systems and the corresponding cycles by computer aided simulations. The benefits of combining the proposed cycles with refrigeration systems and other related issues are also investigated. Several programs have been created in Engineer Equation Solver (EES) for cycle and system simulation and calculation. The properties of the working fluid under different conditions are calculated by Refprop 7.0. A

commercial CFD software (Femlab) has also been used to simulate relevant heat transfer problems and to analyze the air flow field for heat exchangers, which will be further explained in the latter part of the thesis.

4 Cycle Working Conditions

4.1 Carbon Dioxide Transcritical Refrigeration Cycle

For the CO_2 transcritical refrigeration cycle, the working conditions are selected according to the most commonly used working conditions in other research and in CO_2 automobile A/C prototype testing (Man-Hoe, 2004). The evaporation pressure is set to 40 bar and the evaporation temperature will be 5.3 °C accordingly. As is mentioned frequently in other research, there is an optimum gas cooler pressure for the carbon dioxide transcritical refrigeration cycle (Petterssen and Aarlien, 1998; Kauf 1999). For the heat rejection pressure, Liao *et. al.* (2000) proposed a correlation to predict the optimum heat rejection pressure in terms of evaporation temperature and the gas cooler's outlet temperature, which is expressed by Equation 4 -1

$$p_{opt} = (2.778 - 0.0157t_e)t_c + (0.381t_e - 9.34) \quad \text{Equation 4-1}$$

The gas cooler pressure is set to 87 bar, which is the optimum gas cooler pressure calculated by this equation, based on the current evaporation temperature and the 35°C gas cooler outlet temperature.

Moreover, an internal heat exchanger is included in the system to secure a 5 K superheat at the evaporator outlet as a fixed value to ensure there is no moisture at the compressor inlet. Furthermore, the compressor's isentropic efficiency is assumed to be 75% according to the research done by Andrey and Chi-

Chuan (2001). The cycle working conditions are listed in Table 4-1.

Table 4-1 Carbon dioxide transcritical refrigeration cycle operating conditions

Item	Value	Unit
Evaporator pressure	40	bar
Evaporation temperature	5.3	°C
Required cooling capacity	10	kW
Superheat after evaporator	5 (fixed value)	K
Gas cooler pressure	87	bar
Gas cooler outlet temperature	35	°C
Compression efficiency	75%	-

4.2 Carbon Dioxide Transcritical Power Cycle

As mentioned in Chapter 2, the research on the CO_2 transcritical power cycle in low-grade heat source recovery applications is relatively limited. Therefore, several assumptions are needed to specify the cycle working conditions. The gas heater pressure is set to 120 bar and the expansion inlet temperature is related to the heat source temperature. Since this cycle is designed to utilize the energy from a low-grade heat source, 150 °C is assumed as the expansion inlet temperature for the current calculation. Furthermore, the condenser pressure is set to 60 bar with the corresponding condensing temperature at +22 °C. The research on CO_2 pumps is relatively limited compared to the research on CO_2 compressors. However, it is well known that a pump's efficiency is normally higher than a compressor's, mainly due to the smaller volume change during the pumping process than during the compressing process. As a result, the pump's efficiency is assumed to be 0.8 in the current cycle calculations based on Tadano et al.'s research (2000) on CO_2 hermetic compressors, which was done under similar working conditions. The research on carbon dioxide expansion machines

is mainly for use in transcritical refrigeration cycles to replace the throttling valve in order to increase the cycle COP. The expansion efficiency is assumed to be 80% based on findings by several authors (Nickl et al, 2003; Zha et al, 2003; Boewe et al, 2001). In addition, the Internal Heat Exchanger (IHX) effectiveness is assumed to be 90% according to Boewe et al (2001). The cycle operating conditions are listed in Table 4 -2.

Table 4-2 Carbon dioxide transcritical power cycle operating conditions

Item	Value	Unit
Gas heater pressure	120	bar
Condenser pressure	60	bar
Expansion inlet temperature	150	°C
Condensing temperature	21.98	°C
Pumping efficiency	80%	-
Expansion efficiency	80%	-

4.3 Carbon Dioxide Brayton Cycle

As mentioned in Chapter 2. The only difference between carbon dioxide transcritical power cycle and carbon dioxide Brayton cycle is whether there is a part of the cycle located in the sub-critical region or not. If the cycle works as a Brayton cycle, the heat rejection process will take place in the supercritical region and the condenser will therefore be called gas cooler. The cycle operating conditions are listed in Table 4 -3.

Table 4-3 Carbon dioxide Brayton cycle operating conditions

Item	Value	Unit
Gas heater pressure	200	bar
Gas cooler pressure	100	bar
Expansion inlet temperature	200	°C
Gas cooler outlet temperature	40	°C
Compression efficiency	75%	-
Expansion efficiency	80%	-

4.4 Carbon Dioxide Cooling and Power Combined Cycle

The author is not aware of any similar cycle suggested in the literature. Therefore, there are no reference cycle operating conditions available. For the cooling part, the operating conditions are selected according to the operating conditions listed above for the carbon dioxide transcritical refrigerating cycle working conditions. For the power part, the gas heater pressure is selected to 200 bar. The gas cooler pressure is set to 85 bar, which is approximately the optimum gas cooler pressure for the carbon dioxide transcritical refrigeration cycle and the gas cooler outlet temperature is assumed to be 35 °C. Furthermore, the compression and expansion efficiencies are assumed according to the cycles operating conditions listed above. The combined cycle is designed mainly for automobile applications, thus the expansion inlet temperature is assumed to be 350 °C, based on the fact that engine exhaust gas can have a temperature of 500°C at the exhaust gas manifold. The cycle operating conditions are listed in Table 4-4.

Table 4-4 Carbon dioxide cooling and power combined cycle working conditions

Item	Value	Unit
Evaporator pressure	40	bar
Evaporation temperature	5.3	°C
Required cooling capacity	10	kW
Superheat after evaporator	5 (fixed value)	K
Gas heater pressure	200	bar
Expansion inlet temperature	350	°C
Gas cooler pressure	85	bar
Gas cooler outlet temperature	35	°C
Compression efficiency	75%	-
Expansion efficiency	80%	-

5 Heat Exchanger Design

5.1 Description of the Heat Exchanger Calculation Model

The concentric conical shape of the heat exchanger introduces more complexities for the inside (CO_2 side) heat transfer calculation. Due to the specific geometry of the heat exchanger existing heat transfer correlations are not suitable to calculate the tube inside heat transfer for the current heat exchanger, except by employing very complicated numerical solutions. However, the overall objective of the current thesis is system design and validation instead of a detailed heat exchanger design, thus building up a complicated numerical model is therefore beyond the scope of the current work. Furthermore, considering the fact that compared with the CO_2 side heat transfer, the heat exchanger outside heat transfer is the dominating factor for the heat exchanger's heat transfer performance. Therefore, only the dominant side (outside) heat transfer is calculated as a guideline for the preliminary heat exchanger design at the current stage.

According to the design, each heat exchanger plate is composed of three tubes. The outside fluid's flow is crossing the first section of all three tubes at the same time, when reaching the first round of heat exchanger tubes. After passing the first round of tubes, the working fluid will flow further and pass the continued section of the three tubes in the same way. Consequently, the working fluid flow will pass all the sections of the three tubes until it passes the last round of heat exchanger tubes. For the outside heat transfer calculation, the

module can be simplified by spreading the conically shaped heat exchanger plate into a trapezoid shape as shown in Figure 5-1. The airflow is indicated in the figure as an example of heat exchanger outside fluid flow and different colors symbolize different heat exchanger tubes. As shown in the figure, the incoming air will pass the first section of the three tubes at the same time, when it flows over the first round of heat exchanger tubes. After that, the air flow will then pass the second section of three tubes in the same way, when it crosses the second round of heat exchanger tubes. The air will keep flowing and cross the different loops of heat exchanger tubes continually, until it reaches the last section of tubes. For every loop, the CO_2 in each section of heat exchanger tubes is assumed to have the same conditions (i.e. same temperature, same heat transfer characteristics and pressure drop, etc.).

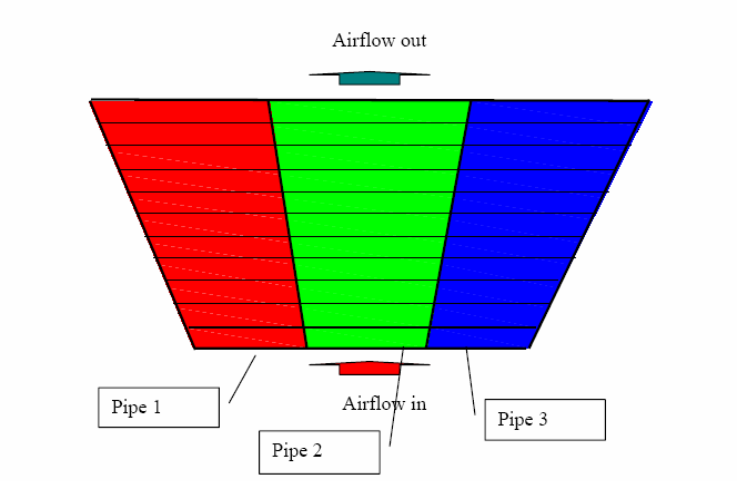

Figure 5-1 Heat exchanger calculation module, schematic 1

When calculating the heat transfer on the outside, due to the characteristics of the heat exchanger geometry, the fluid flow in the rectangular channel, with the channel width being much bigger than the channel height (b>>s), has been assumed as a simplified model for the heat exchanger preliminary design

stage. The scheme is illustrated in the following figure (Figure 5-2):

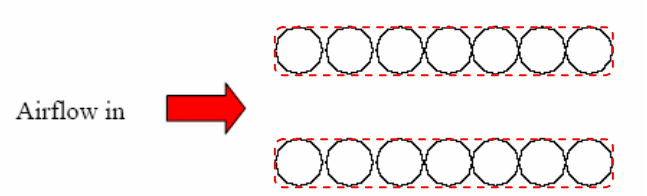

Figure 5-2 Illustration of heat exchanger outside gas flow (side view)

5.2 Basic Correlations

The air mass flow can be calculated by the energy balance as shown below:

$$Q_{power} = \dot{m}_o \times Cp_o \times \Delta t_o \qquad \text{Equation 5-1}$$

$$Q_{power} = \dot{m}_{CO_2} \times \Delta h \qquad \text{Equation 5-2}$$

Where Q_{power} denotes the heat input/output of the heat exchangers (gas cooler, condenser and gas heater), Δt_o is the heat exchanger outside fluid temperature change after passing the heat exchanger. Cp_o is the specific heat of the heat exchanger outside fluid at the mean temperature between the preset inlet and outlet temperature. Δh is the enthalpy difference between the outlet and the inlet refrigerant enthalpies.

As mentioned before, the RANOTOR heat exchanger is designed to work in the laminar flow regime for the heat exchanger outside working fluids. Therefore, the Reynolds number should be calculated and checked to make sure that the flow is well within the laminar region (Re<2300). To calculate the Reynolds number, the velocity of the heat exchanger outside fluid flow is needed and it is obtained by the following equations:

$$\dot{m}_o = \rho_o \dot{V}_o \qquad \text{Equation 5-3}$$

$$\dot{V}_o = u_o \times A_{cross} \qquad \text{Equation 5-4}$$

Where $\dot{V}_o$ is the volume flow of the heat exchanger outside working fluid, $\dot{m}_o$ denotes the mass flow of the outside working fluid and ρ_o denotes density of the outside working fluid. Further, A_{cross} denotes the cross sectional area of the outside working fluid's flow channel (the cross section area between every two plates).

With knowledge of the velocity of the outside fluid flow, the Reynolds number can be calculated accordingly.

$$\mathrm{Re} = \frac{u_o \times d_h}{\nu} \qquad \text{Equation 5-5}$$

Where u_o denotes the velocity of the heat exchanger outside fluid flow, d_h is the hydraulic diameter of the heat exchanger channel, and ν is the kinematics viscosity of the working fluid at the mean temperature.

By checking the Reynolds number, one can verify that the heat exchanger outside flow is laminar. Furthermore, judging by Equation 5-6 and Equation 5-7, it is found that the flow is both in the hydrodynamic entry region and in the thermal entry region (i.e. so-called combined entry length) due to the geometry of the heat exchanger.

$$\frac{x}{d_h} = \frac{\mathrm{Re}}{20} \qquad \text{Equation 5-6}$$

$$Gz^{-1} \equiv \frac{x/d_h}{\mathrm{Re} \times \mathrm{Pr}} = \frac{1}{20} \qquad \text{Equation 5-7}$$

In the above equations, G_z is the Graetz number, x denotes the length of the working fluid's flow and d_h denotes the hydraulic diameter.

Due to the flow conditions, the correlation for calculating the combined entry length heat transfer problem (Equation 5-8), which was developed by Sieder and Tate, can be used for a good approximation of the heat exchanger outside Nusselt number.

$$Nu_o = 1.86 \times \left(\frac{\mathrm{Re} \times \mathrm{Pr}}{L / d_h} \right)^{1/3} \times \left(\frac{\mu}{\mu_s} \right)^{0.14} \qquad \text{Equation 5-8}$$

In which,

$$\mathrm{Pr} = \frac{\mu \times Cp}{k} \qquad \text{Equation 5-9}$$

$$d_h = \frac{4 \times A_{cross}}{P_{cross}} \qquad \text{Equation 5-10}$$

In the above equations, L is the heat exchanger outside working fluid flow length, d_h denotes the hydraulic diameter of the outside fluid's flow channel and Pr is the Prandtl number. A_{cross} denotes the area of the flow channel's cross section and P_{cross} denotes the wet parameter of the cross section. The dynamic viscosity (μ) of the heat exchanger outside working fluid is taken at its mean temperature and μ_s is the dynamic viscosity of the outside working fluid at the heat exchanger's surface temperature.

With knowledge of the Nusselt number, the local heat transfer coefficient for each divided calculation section can be calculated

by the relationship of the heat transfer coefficient and Nusselt number.

$$h_o = \frac{Nu \times k}{d_h} \qquad \text{Equation 5-11}$$

Finally, the temperature of the working fluid after passing one loop of the heat exchanger tubes can be obtained by the energy balance as shown below:

$$h_o \times \left(t_{\text{infinite}} - t_s\right) \times A_o = \dot{m}_o \times Cp_o \times \Delta t_o \qquad \text{Equation 5-12}$$

Where, A_o is the heat exchanger outside surface area, T_s is the heat exchanger surface temperature and $T_{infinite}$ is a variable in the program. $\dot{m}_o$ denotes the mass flow of the heat exchanger outside working fluid and h_o denotes the local heat transfer coefficient for each specific section of the heat exchanger outside working fluid.

The heat exchanger outside fluid pressure drop will decide the fan power, which is also very important for heat exchanger design. The pressure drop is calculated by Equation 5-13.

$$\Delta P = f \times \frac{L}{d_h} \times \frac{\rho}{2} \times u^2 \qquad \text{Equation 5-13}$$

Where f is the friction coefficient, L is the pipe length, d_h is the pipe hydraulic diameter and u is the flow velocity. The density ρ is calculated at the fluid mean temperature.

Several friction coefficients have been suggested by different research for different geometries and for different flow conditions. For laminar flow in slots with small distance in between (b>>s), $\frac{96}{\text{Re}}$ (V.H. Hahnemann and L. Ehret, 1941) can be used for calculating the friction coefficient, which is based on

Hagen-Poiseuilles solution for laminar flow between parallel plates (Equation 5-14).

$$f = \frac{96}{\mathrm{Re}}\left(1 - 1.3553\alpha + 1.9467\alpha^2 - 1.7012\alpha^3 + 0.9564\alpha^4 - 0.2537\alpha^5\right)$$

Equation 5-14

Where *Re* is Reynolds number and α is the aspect ratio, which is defined as the ratio of the channel height to the channel width.

By replacing the friction coefficient with their suggestion, Equation 5-13 can be reformulated in a form as Equation 5-15, which is adopted for the pressure drop calculations in the present work.

$$\Delta P = \frac{12 \times \mu \times L \times \dot{m}}{s^3 \times b \times \rho} \qquad \text{Equation 5-15}$$

In the above equation, *s* denotes the distance between every two heat exchanger plates, $\dot{m}$ is the mass flow of the working fluid, *b* is the width of the flow channels and *L* is the length of the flow channel. The density and the dynamic viscosity are calculated at the fluid mean temperature.

Due to the relatively high system working pressure, the heat exchanger wall thickness is also checked by Barlow's Formula, which is used for calculating the hoop stress of a certain material of a pressurized circular pipe (Equation 5-16).

$$\sigma_1 = \frac{R \times p}{t} \qquad \text{Equation 5-16}$$

Where *t* denotes the thickness of the heat exchanger tube, *p* denotes the tube's inside pressure, σ_1 is the hoop stress for the heat exchanger material and *R* is the heat exchange tube radius.

5.3 Program Description

5.3.1 Evaporator

In the evaporator calculation, the input to design the heat exchanger geometry seeks design effectiveness of the heat exchanger (i.e. the preset working fluid's temperature after passing the heat exchanger), namely: fluid inlet temperature ($t_{fluid\ in}$); preset fluid outlet temperature ($t_{fluid\ out}$), heat exchanger tube's inner diameter, the tube's wall thickness, the tube's first loop diameter, the amount of heat exchanger plates and the distance between every two plates, etc.

The variable $t_{infinite}$ in the calculation loop is first set equal to fluid inlet temperature ($t_{fluid\ in}$), and then the fluid temperature after passing the first loop of heat exchanger tubes can be calculated by Equation 5-12. Furthermore, this temperature will be compared with the preset fluid outlet temperature, which was set as an input to the program, in the if-clause. If this temperature is higher than the preset fluid outlet temperature, $t_{infinite}$ will be set equal to this temperature and thus input into Equation 5-12 again to calculate a new heat source outlet temperature (The temperature after passing two rounds of heat exchanger tubes). The value of t_{wall} is a constant for the evaporator, since the temperature of evaporation is constant (for pure refrigerant regardless of the pressure drop) until the refrigerant totally vaporizes. Following the same procedure, the heat source outlet temperature is calculated until it reaches the preset heat source outlet temperature. Then the calculation loop will stop and the program will export the outputs as: minimum number of plates required to keep laminar flow at the outside of the heat exchanger, the heat source outlet temperature, the number of required tube loops in each heat exchanger plate, approximate heat exchanger size, etc. In addition, the Reynolds number is always checked before the program runs. If the heat exchanger outside fluid's flow is out of the laminar region, a warning will be given by the program to ask the user to reset

the heat exchange geometry in order to keep the heat exchanger outside flow in the laminar region. The program flow chart is shown in Figure 5-3.

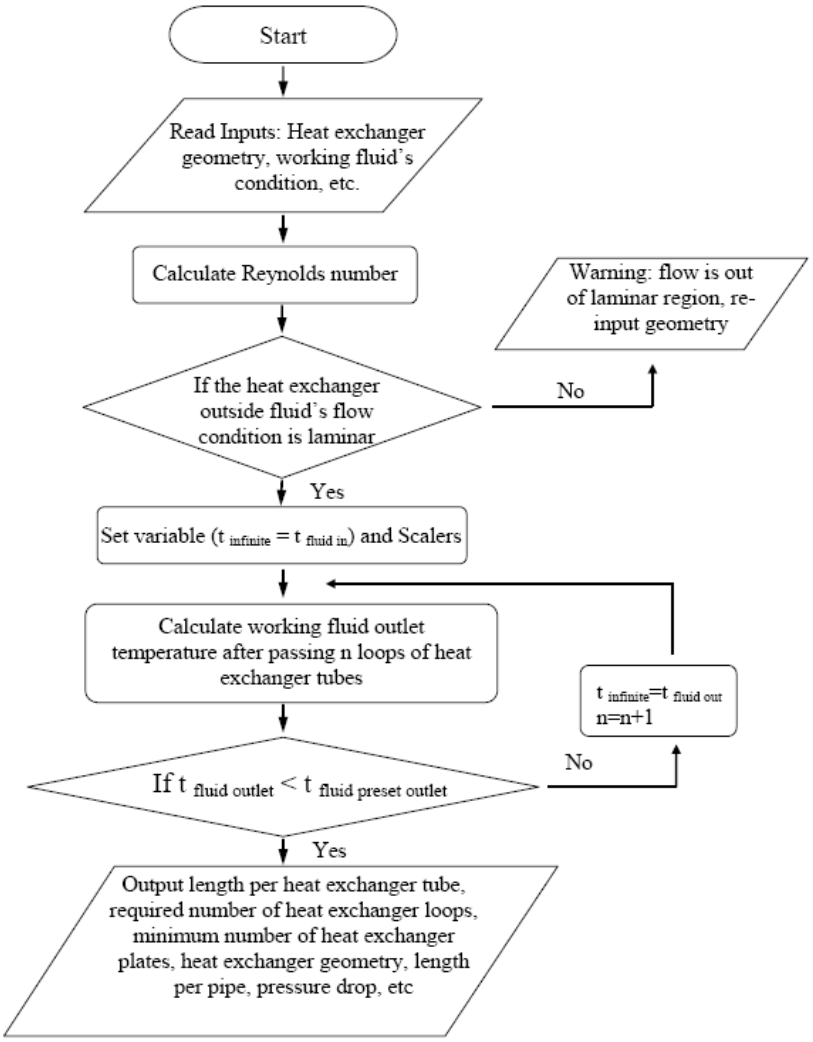

Figure 5-3 Program flow chart— evaporator

5.3.2 Gas cooler

In the gas cooler calculation, an iterative loop is needed. The inputs are fluid inlet temperature, preset fluid outlet temperature, heat exchanger tube inner diameter, the tube's

wall thickness, the tube's first loop diameter, the amount of heat exchanger plates and the distance between every two plates, etc. The Reynolds's number is first checked before the program runs. If the heat exchanger outside flow is out of the laminar region, a warning will be given by the program to ask the user to reset the heat exchange geometry in order to keep the outside flow in the laminar region. Then several variables are set in this calculation, namely: $t_{infinite}$, which equals the fluid inlet temperature; the number of loops at each heat exchanger plate ($n_{loop\ preset}$), which equals 2 as a initial value; Scalars b and n_{loop} are both equal to 1 as initial values, etc. In the inner calculation loop, the fluid temperature after passing one loop of heat exchanger tubes is first calculated and then the number of tube loops on each heat exchanger plate (n_{loop}) is compared with the preset value ($n_{loop\ preset}$) in the if-clause. If n_{loop} is smaller than $n_{loop\ preset}$, the scalars starts to be calculated as $n_{round} = n_{round}+1$, b=b+1, and the value of $t_{infinite}$ is reset as the fluid outlet temperature after passing n loops of heat exchanger tubes, then the calculation loop goes back to Equation 5-12 to calculate a new fluid outlet temperature after passing one more loop of heat exchanger tubes. The calculation loop is kept running until the scalar n_{loop} is bigger than $n_{loop\ preset}$. Then the temperature of the working fluid at this time will be compared with the preset preferred fluid outlet temperature, in the outer calculation loop. If this temperature is smaller than the preferred fluid outlet temperature, all the variables will be set back to the original values; the scalars are reset as $n_{loop\ preset} = n_{loop\ preset} +1$, b=1 and the inner calculation loop will run again to calculate the new fluid outlet temperature.

Following the same procedure, the fluid outlet temperature is iterated until it reaches the preferred fluid outlet temperature that was set as a program's input before. Then the calculation will stop and the program will export the outputs as: minimum number of plates required to keep laminar flow at the heat exchanger outside, the heat source outlet temperature, the number of tube loops in each heat exchanger plate,

approximate heat exchanger size, etc. The program flow chart is shown in Figure 5-4.

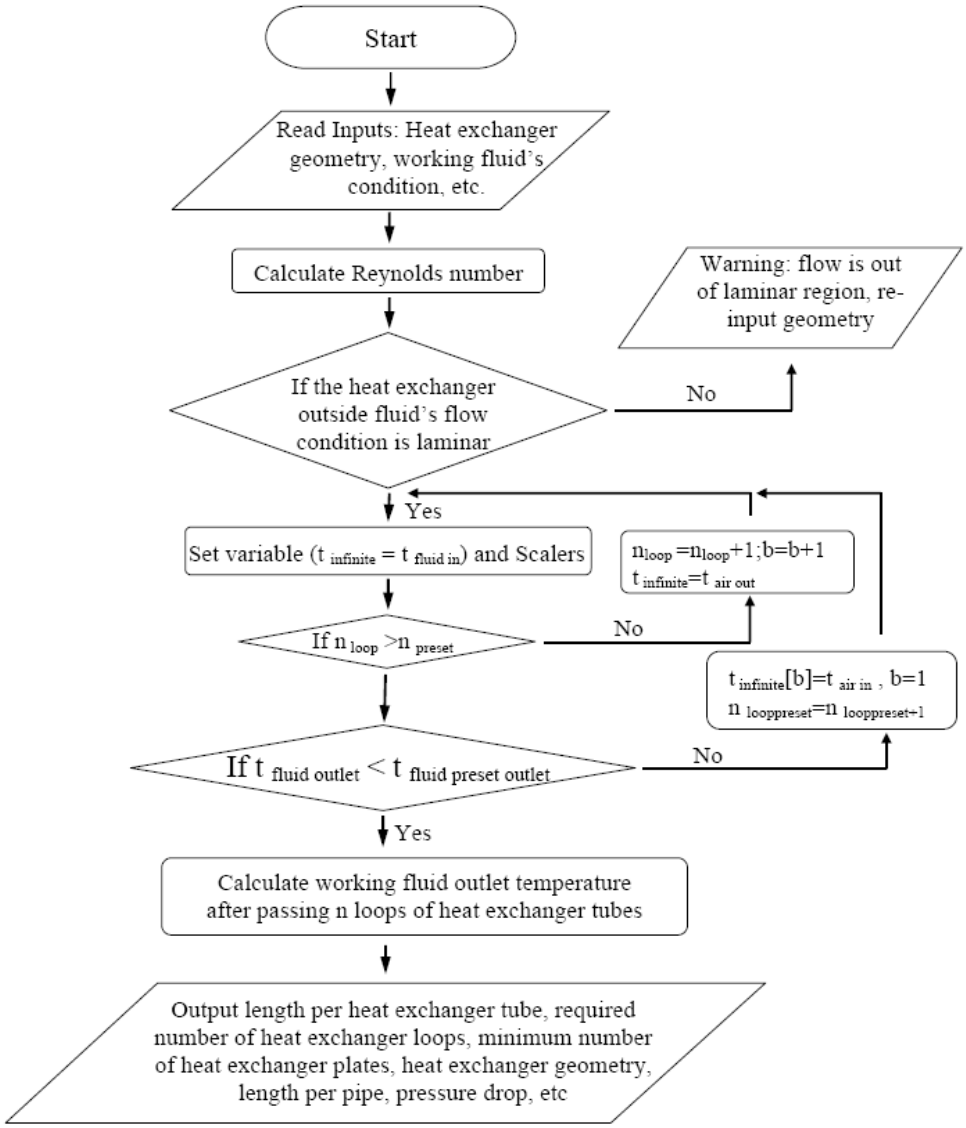

Figure 5-4 Program flow chart— gas cooler

5.3.3 Gas heater

In the gas heater calculation, the inputs are still fluid inlet temperature, preset fluid outlet temperature, heat exchanger

tube inner diameter, the tube's wall thickness, the tube's first loop diameter, number of heat exchanger plates, and the distance between every two plates, etc. First the Reynolds's number is checked before the program runs. If the heat exchanger outside flow is out of the laminar region, a warning sign will be given by the program to reset the heat exchange geometry in order to keep the heat exchanger outside flow in the laminar region. Then several variables are set in this calculation, namely: $t_{infinite}$, which equals the fluid inlet temperature; the number of loops at each heat exchanger plate ($n_{loop\ preset}$), which equals 2 as an initial value; Scalars b and n_{loop} that both equal to 1 as initial values, etc. In the inner calculation loop, the fluid temperature after passing one loop of heat exchanger tubes is first calculated and then the number of tube rounds on each heat exchanger plate (n_{round}) is compared with the preset value ($n_{loop\ preset}$) in the if-clause. If n_{loop} is smaller than $n_{loop\ preset}$, the scalars are then calculated as $n_{loop} = n_{loop}+1$, $b=b+1$, and the value of $t_{infinite}$ is set as the fluid outlet temperature after passing n loops of heat exchanger tubes. Then the calculation loop goes back to Equation 5-12 to calculate a new fluid outlet temperature after passing one more loop of heat exchanger tubes. The calculation loop is kept running until the scalar n_{loop} is bigger than $n_{loop\ preset}$. Then the temperature of the working fluid at this time will be compared with the preset preferred fluid outlet temperature, which was set as an input, in the outer calculation loop. If this temperature is bigger than the preferred fluid outlet temperature, all the variables will be set back to the original values; the scalars are reset as $n_{loop\ preset} = n_{loop\ preset} +1$, $b=1$ and the inner calculation loop will run again to calculate the new fluid outlet temperature. Following the same procedure, the fluid outlet temperature is iterated until it reaches the preferred fluid outlet temperature that was set as an input. Then the calculation will stop and the program will export the outputs as: minimum number of plates required to keep laminar flow at the outside of the heat exchanger, the heat source outlet temperature, the number of tube loops in each

heat exchanger plate, approximate heat exchanger size, etc. The program flow chart is shown in Figure 5-5.

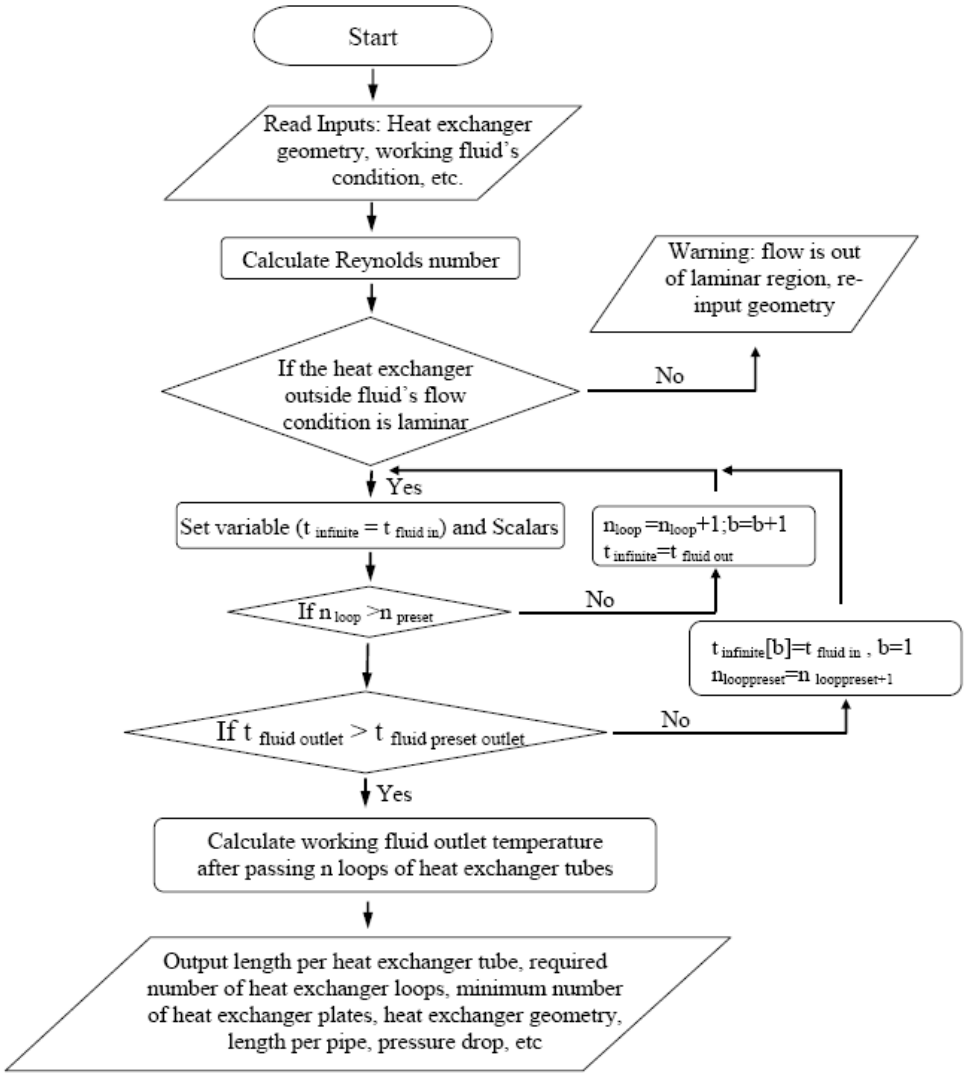

Figure 5-5 Program flow chart— gas heater

5.4 Example of Program Operation Window

The program operation windows are shown in the following figures for different cycles and different heat exchanger design calculations:

5.4.1 Carbon dioxide transcritical refrigeration cycle

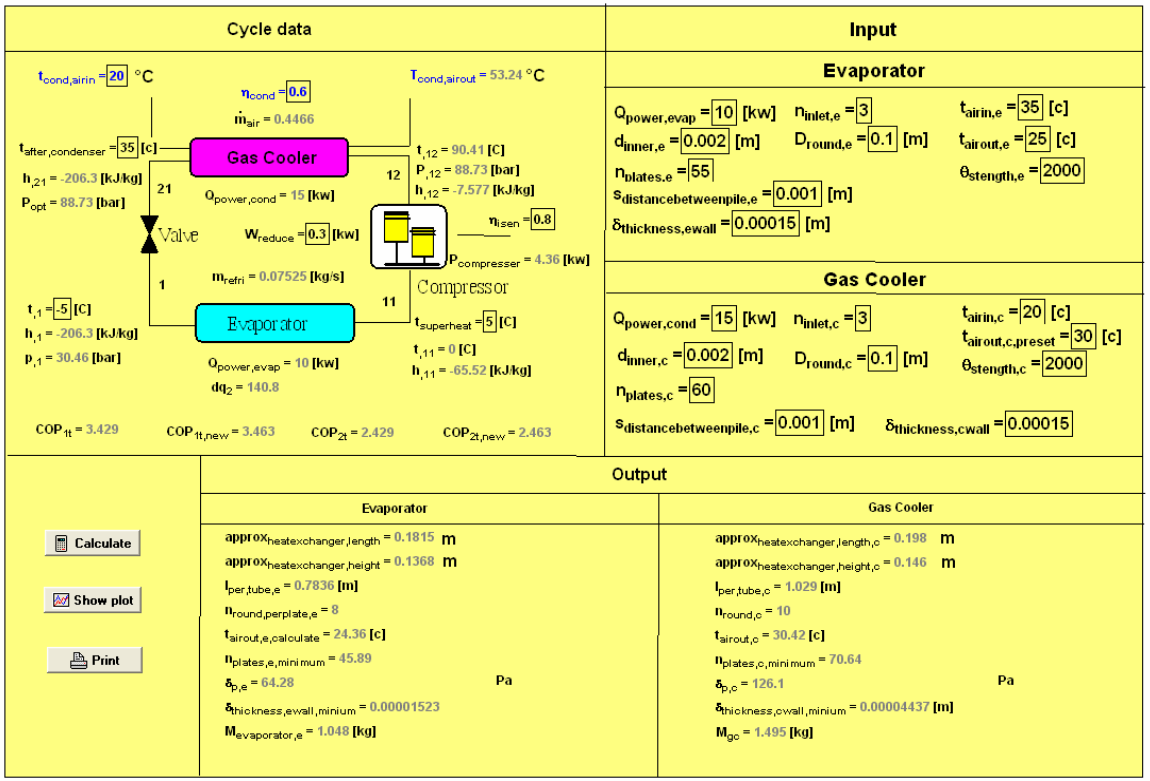

Figure 5-6 Program operation window— CO_2 transcritical refrigeration cycle

5.4.2 Carbon dioxide transcritical power cycle

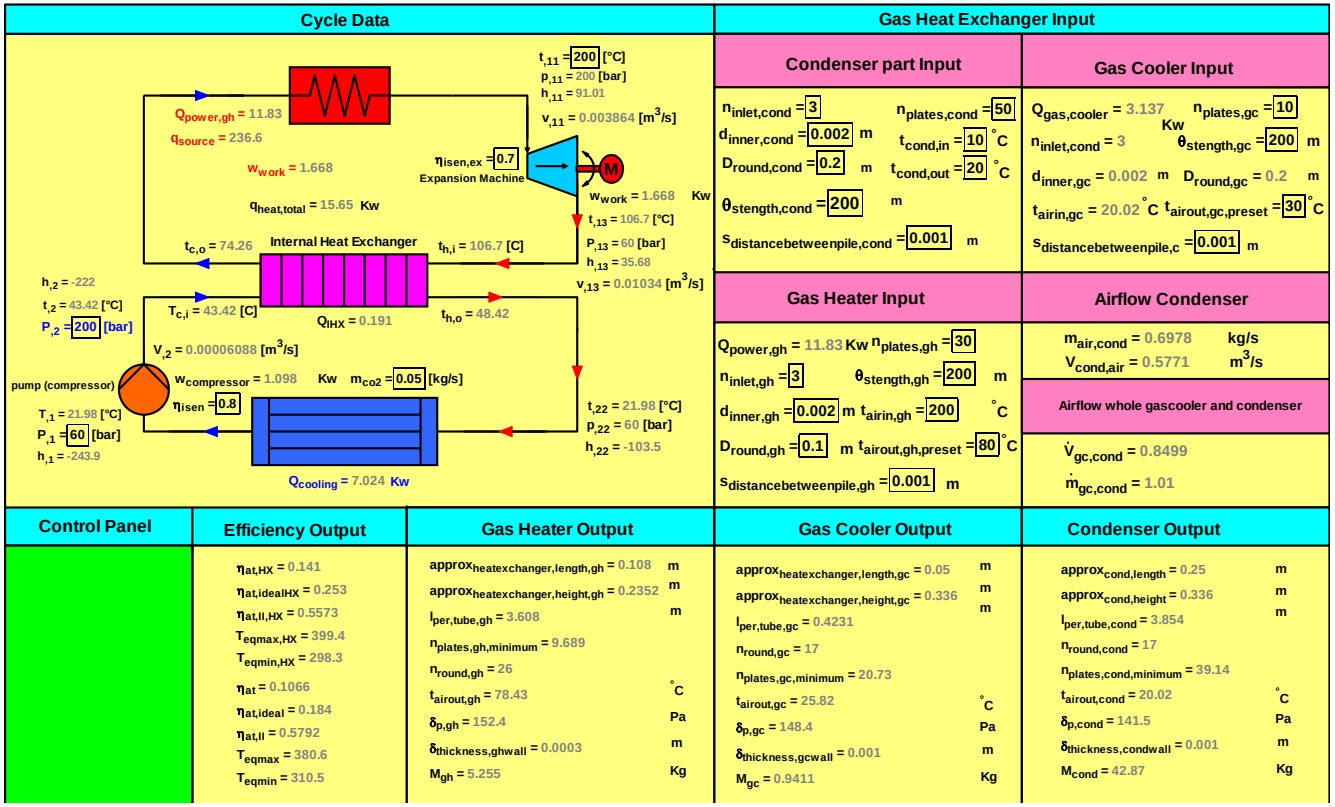

Figure 5-7 Program operation window—CO_2 transcritical power cycle

5.4.3 Carbon dioxide cooling and power combined cycle

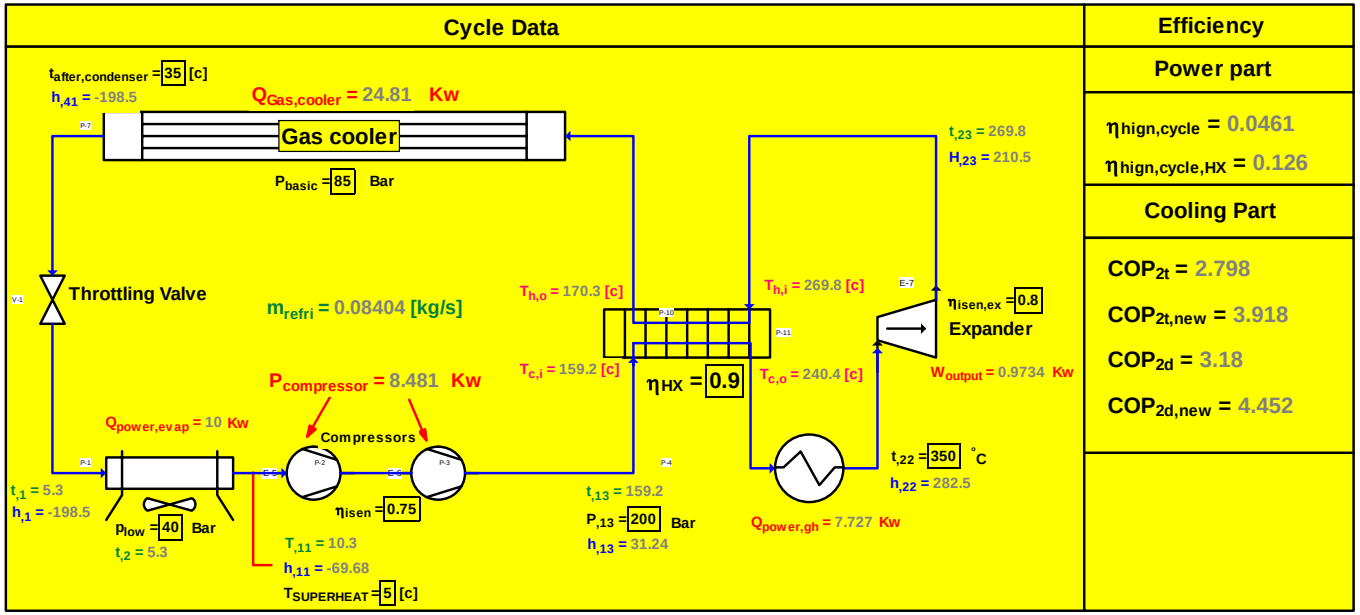

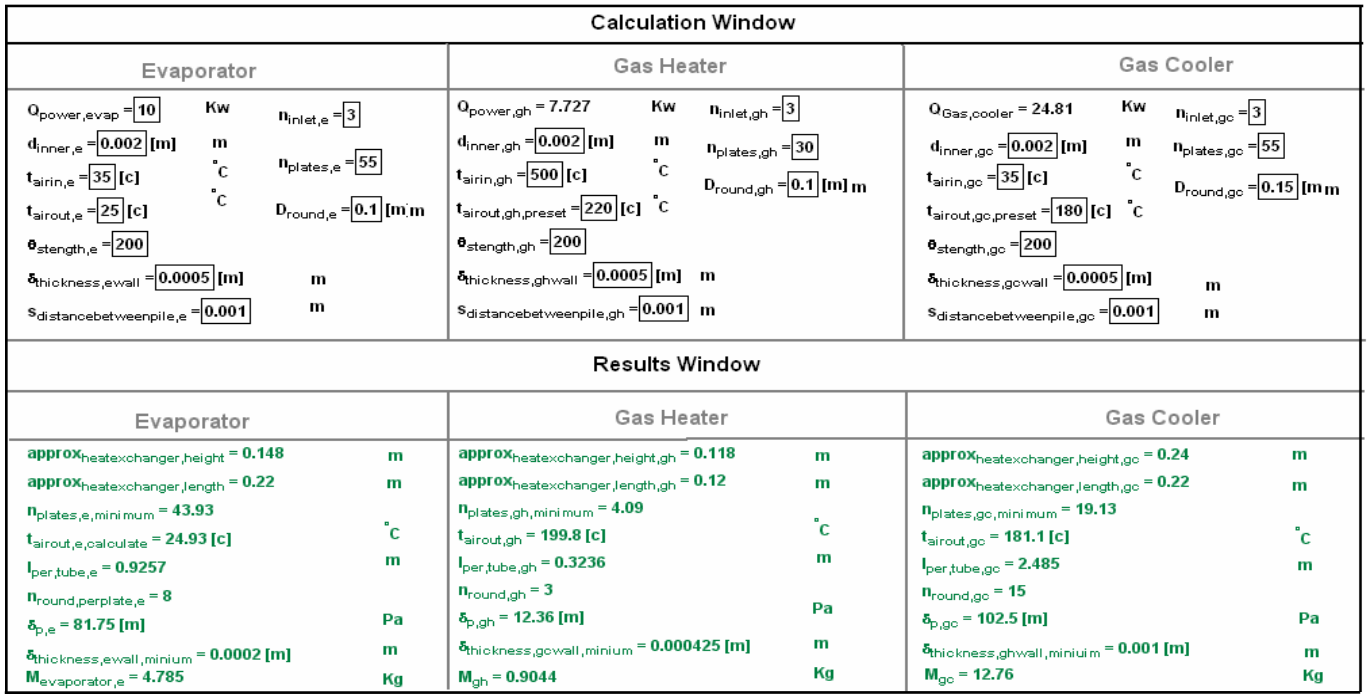

Figure 5-8 Program operation window—CO_2 cooling and power combined cycle

5.5 Results

The results will vary according to different designs and different application purposes, thus it is hard to give a general result here. To give a general idea about the cycle performance, the cycle performance under the basic cycle working conditions described in chapter 4 are listed in Table 5-1.

Table 5-1 Cycle performance

Items	COP	COP $_{new}$[7]	Efficiency
CO_2 transcritical refrigeration cycle	3.18	—	—
CO_2 transcritical power cycle	—	—	11.6%
CO_2 Brayton cycle	—	—	10.3%
CO_2 combined cycle	3.18	4.45	12 .6% [8]

A more detailed discussion about the cycle performance and different factors' influences on the cycle performance is given in Chapter 7.

Some sketches according to several design calculations are also shown below to give a general idea about the heat exchanger geometry.

7 COP $_{new}$ is calculated by the ratio of cycle cooling capacity to the cycle new compression work, which is the original compression work minus the net work provided by the combined cycle power part, see page 23 for a definition.

8 This efficiency is the combined cycle power part efficiency

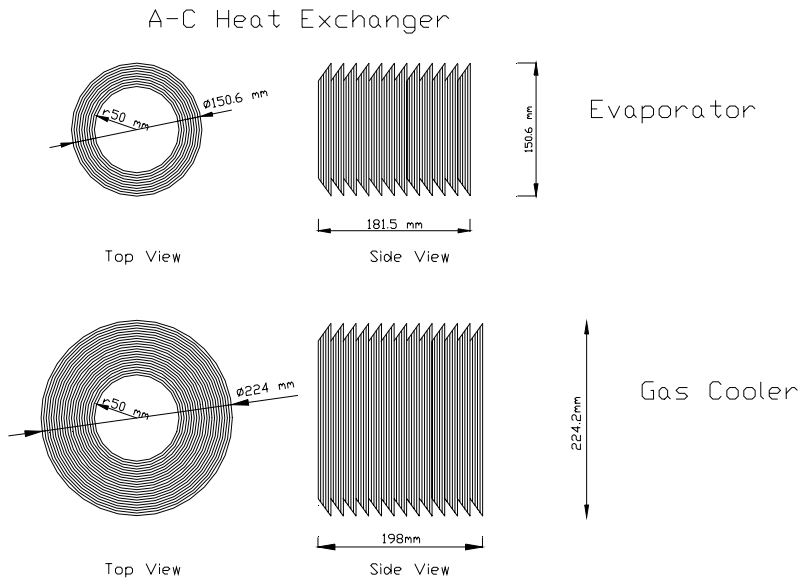

Figure 5-9 Carbon dioxide transcritical refrigeration cycle's heat exchanger

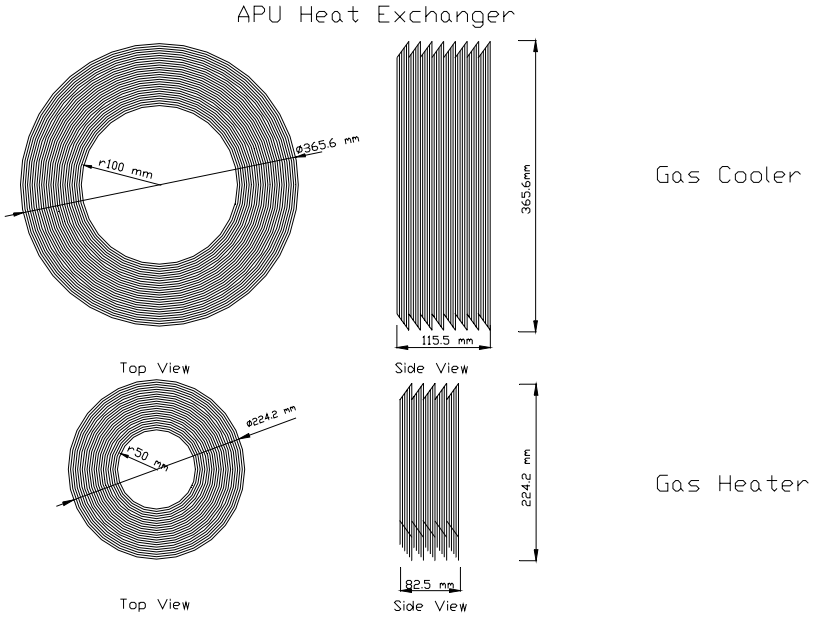

Figure 5-10 Carbon dioxide transcritical power cycle's heat exchangers

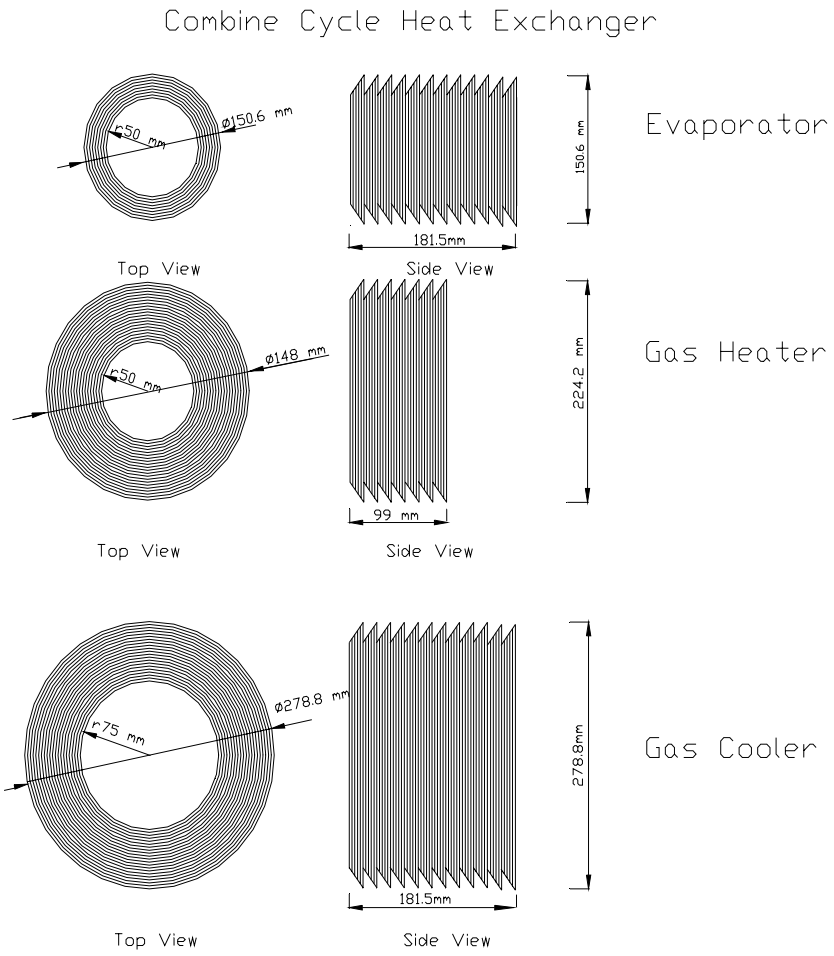

Figure 5-11 Carbon dioxide refrigeration and power combined cycle's heat exchanger

6 CFD Analysis

Femlab was used at an early stage of this study to predict the flow field between the heat exchanger plates and to analyze how heat conduction along the heat exchanger influences performance.

6.1 The Flow Field

A 2D geometry module was developed in Femlab to simulate the flow field between the heat exchanger plates. The geometry was drawn according to the result from heat exchanger design calculations in the previous section. Thanks to the symmetrical shape of the heat exchanger plates, simulating two heat exchanger plates is enough to predict the flow conditions between every two heat exchanger plates. Furthermore, an even simpler module could be realized by cutting through the center line of the heat exchanger tubes.

The multiphysics module, which includes conduction, convection and non-isothermal, incompressible flow modules, is employed to simulate the flow field between the heat exchanger plates. For the conduction and convection module, the initial temperate of gas flow domain is set to 23 °C and the gas properties are selected according to this temperature. For the domain of heat exchanger tubes, the temperature of each tube is set according to the result from the EES calculation and copper is selected as tube material. Exhaust inlet boundary is set to exhaust gas inlet temperature (200 °C in the example figure) and outlet boundary is selected to convective flux. Further, all the boundaries of the heat exchanger tube walls are set to temperatures, whose values are selected based on the temperatures of the corresponding domain and all the outer

boundaries of the module geometry are set as adiabatic. The non-isothermal, incompressible flow module assumes that the expansion work done by the gas is negligible, that the variations in temperature are obtained through external heating, and that the fluid is an ideal gas. In this module, the initial flow velocity is set to zero. The inflow boundary is set as velocity boundary, whose value is based the results from the EES calculation. The symmetrical gas flow boundary in the horizontal flow domain is set to slip symmetry and all other flow boundaries are set to no slip.

Triangle mesh is automatically generated in Femlab and the initialized mesh consisted of 2466 elements, which is shown in the left part of the following figure. In addition, the tube connecting corner is specially treated with a refined mesh, due to the fact that vortexes may occur at these corners. The refined mesh consisted of 4887 elements and the final mesh is shown in the right part of Figure 6-1.

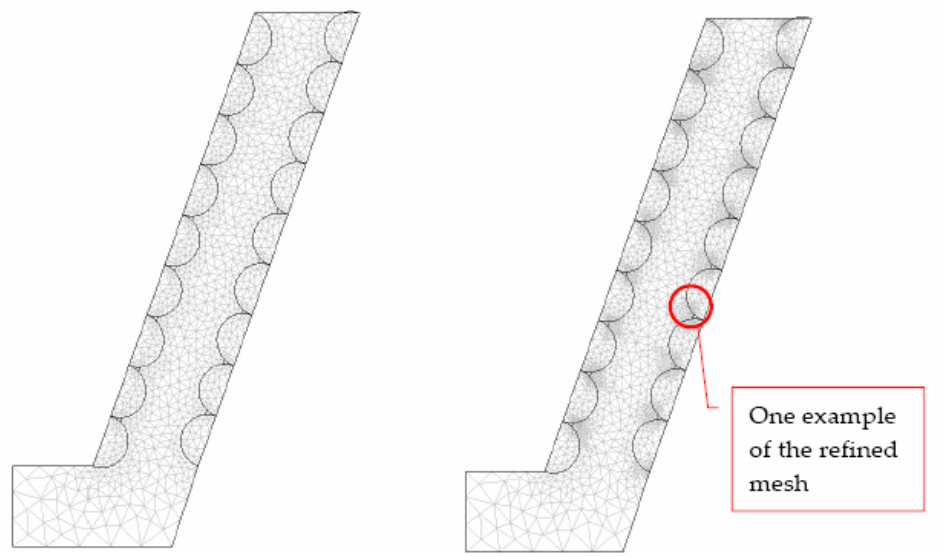

Figure 6-1 Coarse and fine meshes of the 2D geometry of heat exchanger plates

Examples of the results for the temperature and velocity fields are plotted in Figure 6-2, in which the surface color shows the temperature field and the streamline shows the velocity field. Furthermore, a contour plot is also plotted in Figure 6-3 to show the flow pattern and velocity of the flow.

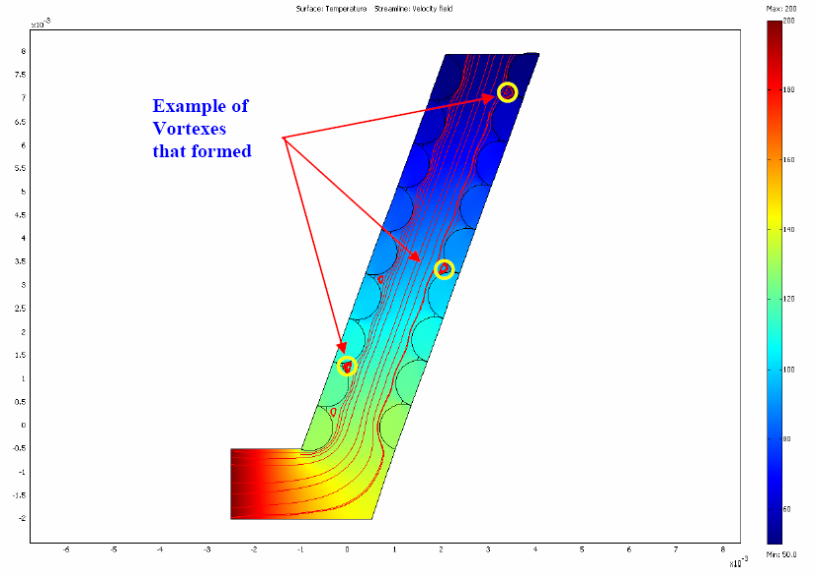

Figure 6-2 2D surface and streamline combined plot for both temperature change and velocity field of the heat exchanger

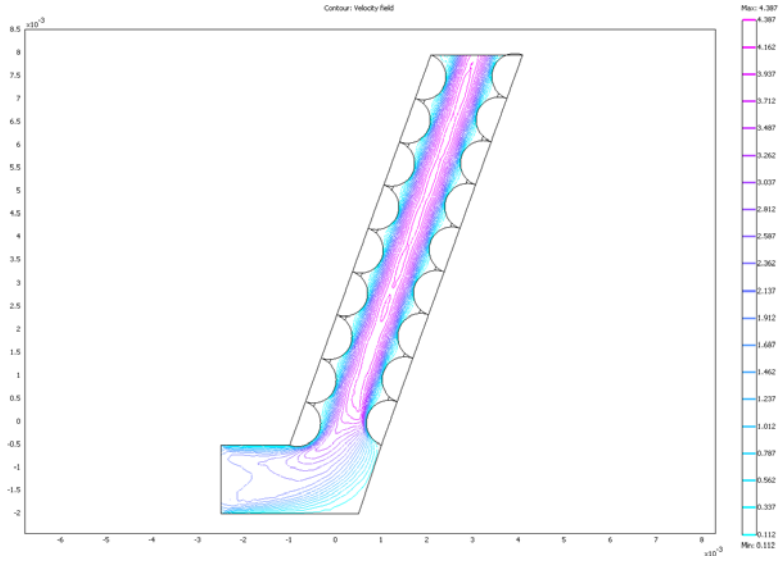

Figure 6-3 2D contour plot for velocity field of the heat exchanger plate

From the results, it is found that the temperature change of the heat exchanger outside working fluid is in the range of what was expected from the calculation results in the EES program. Vortexes are detected and it is also found that the formation and the location of the vertex are greatly related to the heat exchanger plate angles. The Reynolds number has been checked and it is within the laminar region.

6.2 The Influence of Conduction

The proposed heat exchanger is working with a large temperature gradient along the flow direction, thus the conduction inside the heat exchanger material may have a big influence on the heat exchanger performance and cause so-called "thermal short circuiting". Therefore, a 3D module has been built in Femlab to check the influence of the conduction inside the material on the heat exchanger temperature profile. Due to the computer limitations, only a section of the heat exchanger is simulated at the current stage. The 3D geometry is built based on the calculation results from the EES program, which is shown in Figure 6-4. In the figure, the red part is the heat source flow path (exhaust gas was used as an example in the module), the green part is the heat exchanger tube material and the blue parts are the heat exchanger tubes.

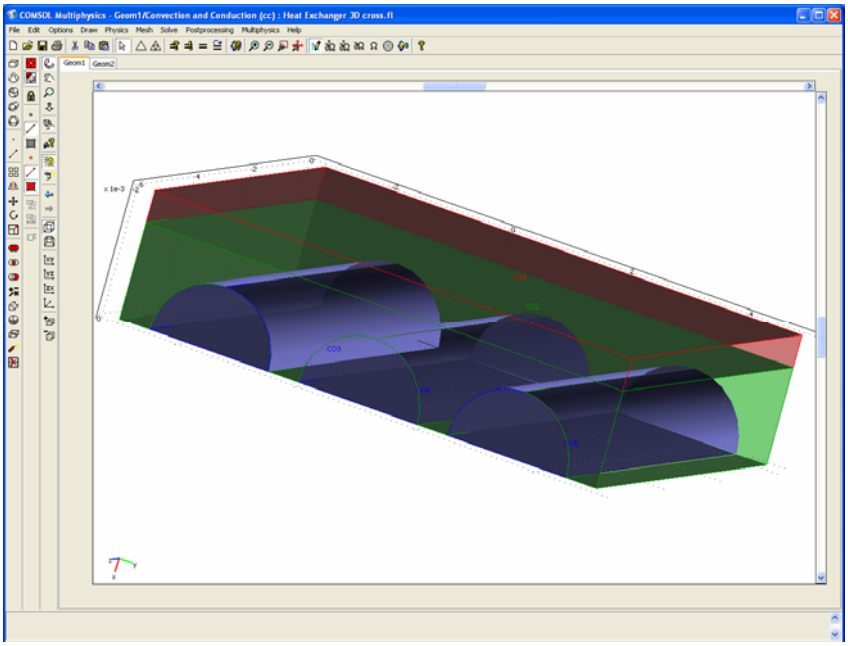

Figure 6-4 A 3D geometry for one section of the heat exchanger plates

The multiphysics module which includes conduction, convection and non-isothermal, incompressible flow modules is still employed in this simulation. For the conduction and convection module, the initial temperate of gas flow domain is set to 23 °C and the properties are selected according to this temperature. Copper is selected for the heat exchanger tube domain with initial temperature 23 °C. The carbon dioxide flow domain (blue part) is set to different temperatures according to the results from EES calculation and the properties are selected according to the preset temperature. The inflow boundaries for exhaust gas and carbon dioxide are set to temperatures, which is based on the calculation in EES and the outflow boundaries are set to convective flux. All the other inner boundaries are set to continuity and all the outer boundaries of the module geometry are set to thermal simulation. For the non-isothermal flow module, the initial flow velocity is set to zero. The inflow boundaries for exhaust gas and carbon dioxide are set as inflow velocity boundaries, whose values are based the results from EES calculation. The symmetrical gas flow boundaries in the

flow domain are set to slip/symmetry and all other flow boundaries are set to no slip. For the settings mentioned, the counter flow condition is set.

The mesh is automatically generated in Femlab and the initialized mesh consists of 10958 elements, shown in Figure 6-5. The mesh is not refined because the results already show that the conduction in the heat exchanger material indeed does influence the heat exchanger's temperature profile.

The temperature boundary, slice and isosurface plots are shown in Figure 6-6 thru Figure 6-8 respectively. It can be noticed from these figures that the temperature profile of the heat exchanger is influenced by the conduction inside the material. In future studies, the importance of this phenomenon will be further investigated. However, the influence of the material's conduction can also be alleviated by changing the geometry of the heat exchanger.

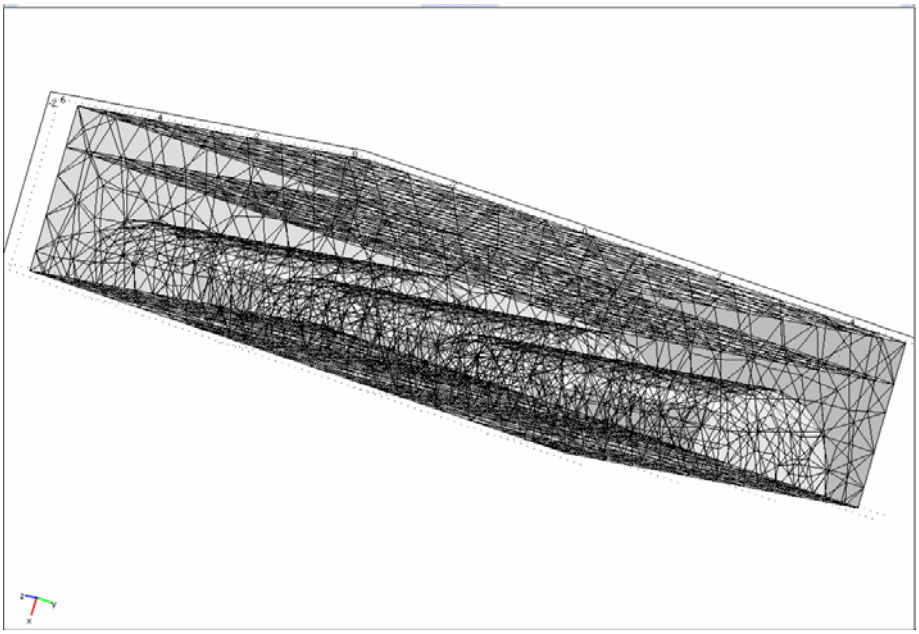

Figure 6-5 Mesh of the 3D geometry for one heat exchanger section

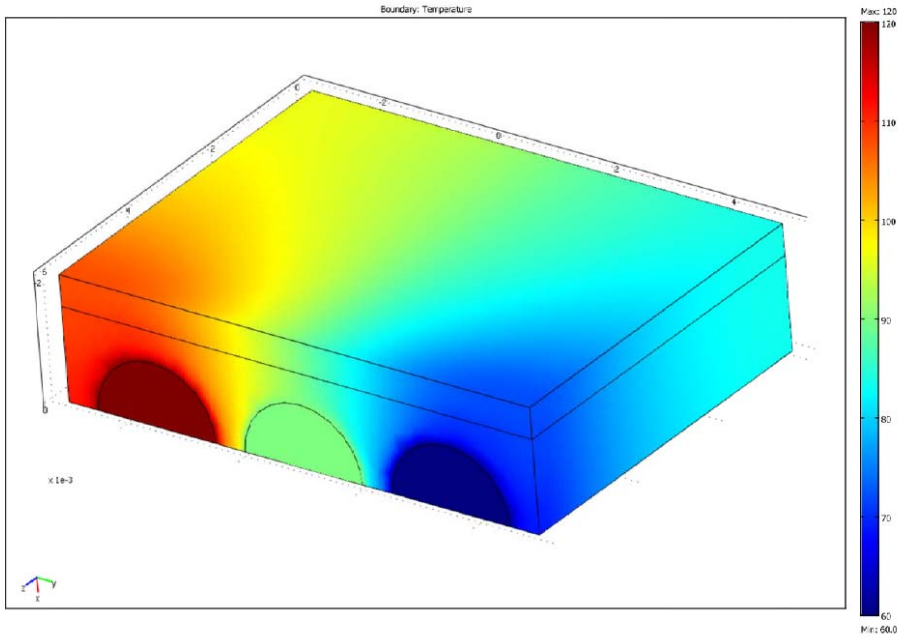

Figure 6-6 3D temperature boundary plot of the heat exchanger

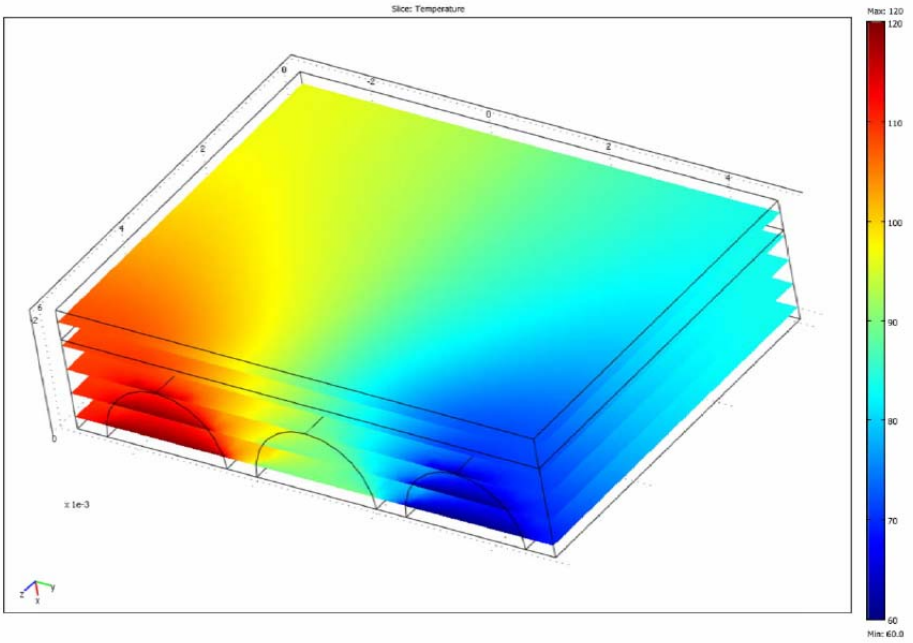

Figure 6-7 3D temperature slice plot of the heat exchanger

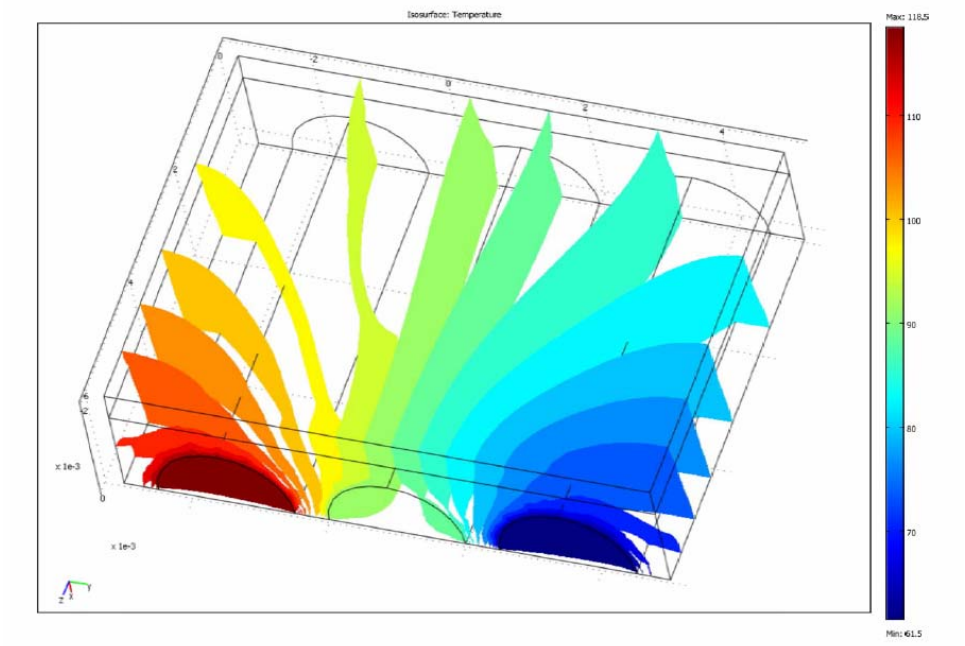

Figure 6-8 3D temperature isosurface plot of the heat exchanger

7 Discussion, Conclusion and Further Work

7.1 Discussion

According to the cycle working conditions, power cycles can be divided mainly into three groups. They are: (i) the Sub-critical cycles, which means both the cycle's heating and condensing processes will be partly located in the sub-critical region; (ii) the transcritical cycles, which means part of the cycle will be located in the supercritical region, while part of the cycle will be located in the sub-critical region; and (iii) the Brayton cycles, which means the entire cycle is located in the supercritical region. Due to the low critical point of carbon dioxide (73.8 bar and 31.1°C), the carbon dioxide power cycle will be a transcritical cycle or Brayton cycle accordingly.

Thermodynamically, the larger the temperature difference between the cycle's heat absorbing temperature and the cycle's heat rejecting temperature is, the higher the cycle efficiency will be. From this point of view, for the same heat absorbing temperature, the CO_2 transcritical power cycle will achieve a higher efficiency than the CO_2 Brayton cycle if a low temperature heat sink is available. To achieve a satisfying efficiency of the carbon dioxide Brayton cycle, a relatively higher heat source temperature is needed, which will be out of the low-grade heat source range.

For supercritical carbon dioxide, the iso-bars are relatively sparse in the area near the critical point, but become dense in both low and high temperature areas. Furthermore, the temperature and pressure are not linked to each other in the

supercritical region. Therefore, there is always an optimum pressure for a certain carbon dioxide transcritical cycle, which is influenced by many factors, mainly: internal heat exchanger effectiveness, the gas cooler outlet temperature as well as the compressor and expander's specifications. By plotting the expansion inlet temperature *vs.* cycle efficiency for a given pump efficiency with various expansion efficiencies, and by plotting the expansion inlet temperature *vs.* cycle efficiency for a given expansion efficiency with various pump efficiencies (Figure 7-1 & Figure 7-2), it is found that the cycle efficiency will improve with increasing of the expansion inlet temperature. However, after a sharp increase at the beginning, the efficiency slope becomes flat over a large temperature range, which shows that it is more effective to improve the cycle efficiency by increasing the expansion inlet temperature over the low temperature region, rather than further increase it to the high temperature region[9]. Thus the proposed CO_2 transcritical power cycle is more suitable for converting the low-grade energy in the exhaust gas into useful energy. These figures also illustrate that the efficiencies of expansion and compression units will have a crucial impact on the cycle efficiency.

9 This result is based on the given gas heater pressure, which is in the lower pressure region compared with carbon dioxide Brayton cycle. In the current research in utilizing the low-grade heat source by transcritical power cycle, only relative lower gas pressure is considered, for the consideration of system safety, etc.

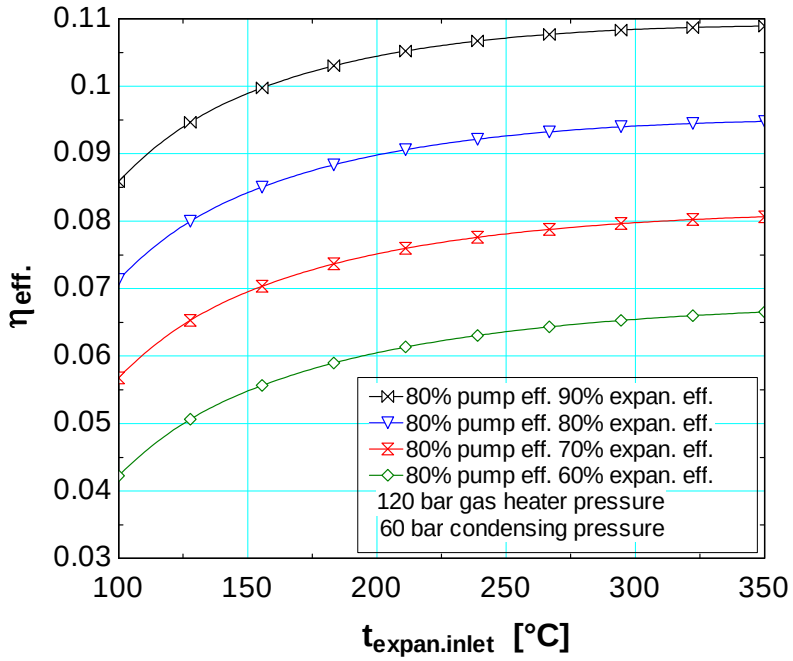

Figure 7-1 Carbon dioxide transcritical cycle efficiency vs. expansion inlet temperature against various expansion efficiencies (from EES, basic cycle without IHX)

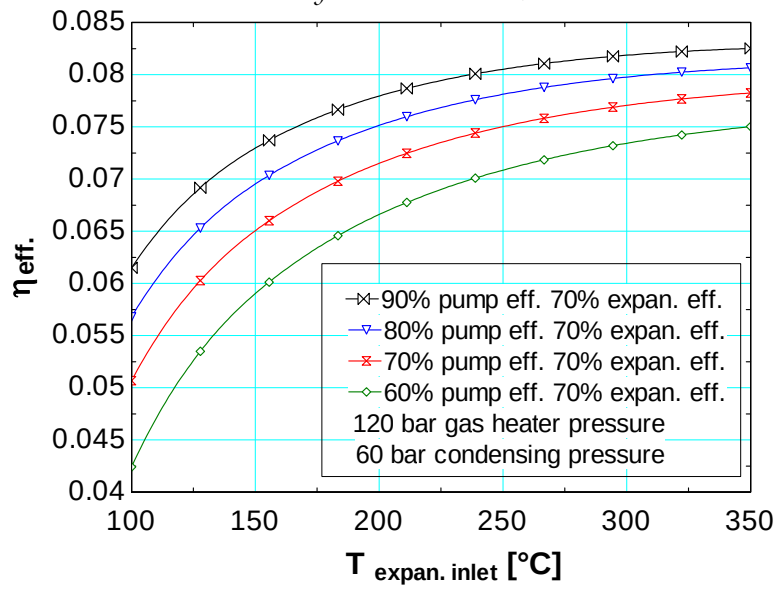

Figure 7-2 Carbon dioxide transcritical cycle efficiency vs. expansion inlet temperature against various pump efficiencies (from EES, basic cycle without IHX)

Furthermore, by plotting the influence of the cycle pressure ratio on the cycle efficiency for different expansion inlet temperatures (Figure 7-3), it is clearly shown that there is an optimum pressure ratio for a certain expansion inlet temperature and condensing temperature.

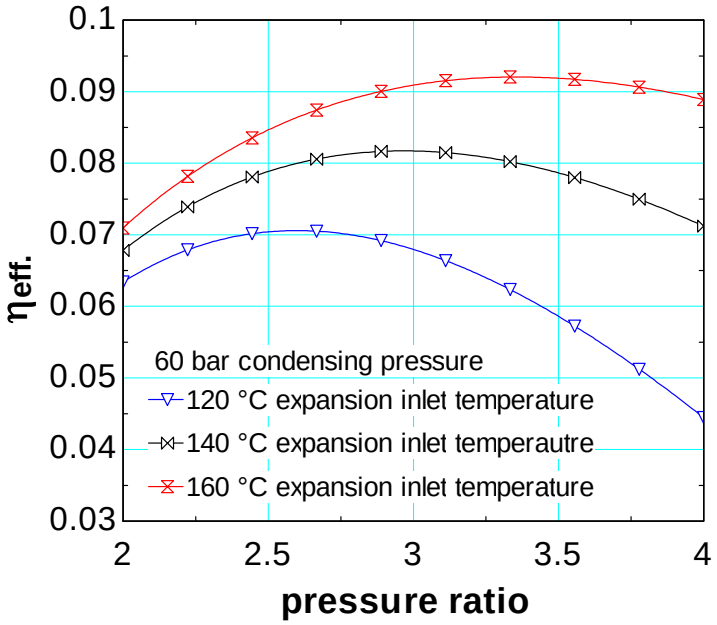

Figure 7-3 The influence of pressure ratio on carbon dioxide transcritical cycle efficiency (from EES, basic cycle without IHX)

Moreover, unlike other power cycles, the carbon dioxide transcritical power benefits strongly from internal heat regeneration. Therefore, the internal heat exchanger (regenerator) will have a crucial influence on the cycle performance, which is shown in Figure 7-4.

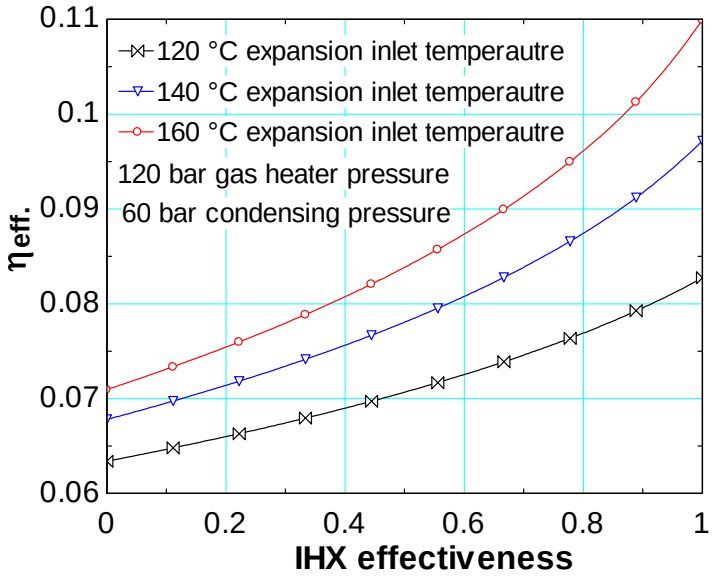

Figure 7-4 The IHX effectiveness' influence on carbon dioxide transcritical cycle efficiency (from EES)

The proposed CO_2 cooling and power combined cycle (system) is suitable for automotive applications, where the automobile engine will give off a lot of waste heat. The cooling part of the combined cycle will have an optimum gas cooler pressure for certain working conditions. The cooling part COP of the combined cycle is plotted against different gas cooler pressures while keeping other cycle working conditions constant as proposed above for the basic cycle (Figure 7-5). From the figure, one can see that at the optimum gas cooler pressure, the improvement of the cooling cycle's COP is tremendous (e.g. around 40% of the basic cycle's COP) and the enhancement of COP is different for different gas heater pressures. It is also found that the optimum gas cooler pressure for the combined cycle's cooling part (i.e. to achieve the highest $COP_{new,}$ after transferring the power gained form the cycle's power part to the cooling part) will remain the same as that for the basic transcritical cooling cycle (around 85 bar for the proposed working conditions).

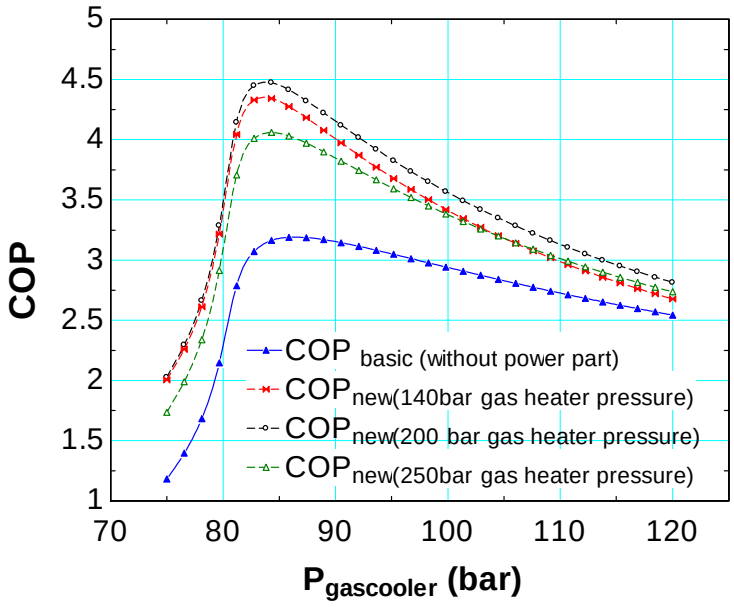

Figure 7-5 The COP of the cooling part of the combined cycle vs. different gas heater pressures (from EES)

7.2 Conclusion

In the current thesis, several carbon dioxide novel cycles and systems have been analyzed for their potential in utilizing the energy from low-grade heat sources. The analyze of different systems and corresponding cycles suggest that the proposed cycles and systems will be a new way to make use of previously unexploited energy sources, which could otherwise be difficult with traditional power cycles.

When utilizing a low-grade heat sources, the carbon dioxide transcritical power cycle will achieve higher efficiency, especially in applications where there is also a low-temperature heat sink available. On the contrary, the carbon dioxide Brayton cycle will achieve lower efficiency, but is more suitable when there is no low-temperature heat sink available. The carbon dioxide cooling and power combined cycle is a newly proposed idea, which is energy efficient when there is both cooling and power required or for automobile applications.

7.3 Further Work

In regard to further work, experimental investigation of the proposed systems will be performed. The sketch of the planned final test rig is shown in Figure 7-6, in which the air loop is used to simulate the low-grade heat source by heated air. The air is circulated in the air loop and heated up by the electrical heater. It then goes through the CO_2 gas heater thus heating up the working fluid before entering the expander. The black line in the sketch is the CO_2 loop (the cycle). After being heated the CO_2 will expand in the expansion machine and produce mechanical work. After passing the internal heat exchanger (regenerator) the working fluid goes to the condenser and is cooled by the cooling water. After the gas/liquid separator, the CO_2 will be pumped by the CO_2 pump to higher pressure. The gas enters the heater after passing the regenerator. The condenser part in the test rig can be used for CO_2 two-phase condensing (in tube cooling) characteristics investigation as well as CO_2 heat exchanger testing.

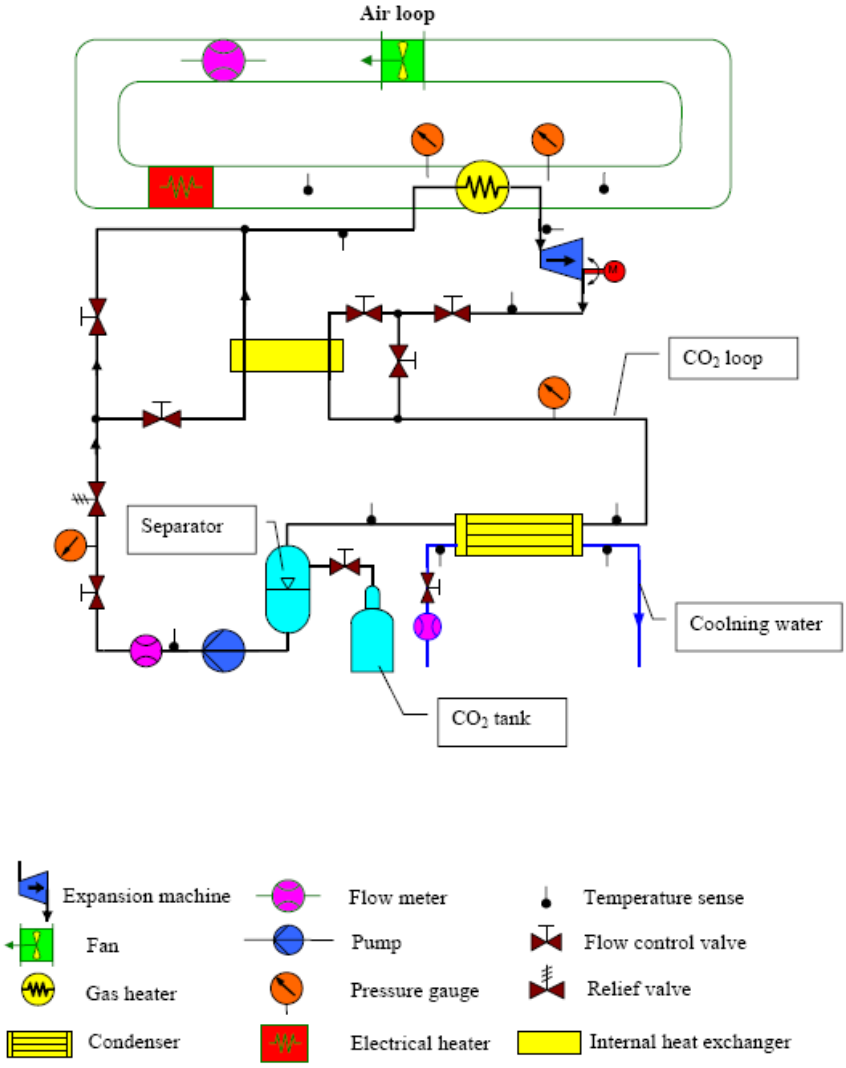

Figure 7-6 Schematic layout of the CO_2 power system test rig

The experimental investigation of the proposed system will be performed in different stages:

1) Heat exchanger testing and validation

During this stage, the designed RANOTOR heat exchanger will be tested, validated and optimized. The heat transfer scheme of supercritical carbon dioxide in the heat exchanger will also be studied and analyzed. At the same time, design and modification of existing pumps and expanders will be performed to make them suitable for the proposed system.

2) System performance testing and validation

Experimental testing on the whole system performance, which includes system performance testing, validation and working condition optimization, will be performed. Later on, different components' performances will be further studied. Data will be gathered for the next stage of different components optimization.

3) System working conditions optimization

Different components in the system will be optimized and the system performance will be tested to get the optimized working point for different working conditions (pressure optimization, etc.). The design of the heat exchanger, the pumps and expanders will also be improved in order to achieve better system performance.

Research on heat transfer and pressure drop characteristics of supercritical and sub-critical carbon dioxide in heating and cooling processes, as well as their influences on the heat exchanger's heat transfer performance will be conducted throughout all three stages.

8 References

ASHRAE Handbook 1993, Fundamentals, SI edition

Boewe, D.E., C.W. Bullard, Yin J.M. and P.S. Hrnjak, 2001, "Contribution of Internal Heat Exchanger to transcritical R-744 Cycle Performance", *HVAC&R Research*, VOL. 7 NO. 2

Chang, H., 2002, *Development of a Supercritical Carbon Dioxide Brayton Cycle: Improving PBR Efficiency and Testing Material Compatibility*, Idaho National Engineering and Environmental Laboratory (INEEL)

DiPippo, R., 2004, "Second Law assessment of binary plants generating power from low-temperature geothermal fluids", *Geothermics*, 33 (2004) 565–586

Dostal, V. M.J. Driscoll, P. Hejzlar, Y. Wang, 2004. "Supercritical CO_2 cycle for fast gas-cooled reactors", *Proc. of ASME Turbo Expo 2004, Power for Land, Sea, and Air*

Energy in Sweden 2004, Report from Swedish Energy Agency

European Forum for Renewable Energy Sources,2003, http://www.eufores.org/index.php?id=30#_Toc106430664

Feher, E.G, 1967, "The Supercritical thermodynamic power cycle", *Energy Conversion*, Vol.8.pp 85-90

Fukuta, M., Yanagisawa, T., and Radermacher, R., 2003, "Performance prediction of vane type expander for CO_2 cycle", *Proc. of 21st IIR Internal congress of refrigeration 2003*, ICR0251.

Hahnemann, V. H., and L.Ehret, 1941, "Der druckverlust der laminaren strömung in der anlaufstrecke von geraden, ebenen spalten", *Jahrbuch 1941 der deutschen luftfahrtforschung.*

Hung, T.C., 2001, "Waste heat recovery of organic Rankine cycle using dry fluids", *Energy Conversion and Management* 42 (2001) 539-553.

Incropera, F.P. and D.P. DeWitt, 2001, *Fundamentals of Heat and Mass Transfer 5th edition*, ISBN 0-471-38650-2

Kauf, F, 1999, "Determination of the optimum high pressure for trasncrtitical CO_2 refrigeration cycles", *International Journal of Thermal Sciences,* (1999) 38, 325-330.

Kays, W. M., 1955, ''Numerical Solutions for Laminar Flow Heat Transfer in Circular Tubes,'' *Trans. ASME*, 77, pp. 1265–1274.

Kim, M-H., Pettersen, J., Bullard, C.W., 2004, "Fundamental process and system design issues in CO_2 vapour compression systems", *Progress in energy and combustion science,* 30(2004):119-174

Liao, S.M., T.S Zhao, A. Jakobsen, 2000, "A correlation of optimum heat rejection pressures in transcritical carbon dioxide cycles", *Applied Thermal Engineering,* 20 (2000) 831-841.

Nickl, J., G. Will, W.E. Kraus and H. Quack, 2003, "Third generation CO_2 expander", *Proc. of 21st IIR Internal congress of refrigeration*, ICR0571.

Pettersen, J., and Aarlien, R., 1998, "Progress in vapor compression systems", *Thermal science and engineering*, Vol. 6, No1

Rozhentsev, A., and Wang, C-C., 2001, "Some design features of a CO_2 air conditioner", *Applied Thermal Engineering,* 21 (2001):871-880.

Shah, R.K. et.al, 1991, *Heat Exchanger Engineering Volume 2—Compact Heat Exchangers,* In: E.A.Foumeny and P.J.Hegys**,** Ellis Horwood, ISBN 0-13-382391-1, PP.1-27

Tadano, M., T. Ebara and A. Oda, 2000, "Development of the CO_2 hermetic compressor", *Proc. of the 4th IIR-Gustav Lorentzen Conference on Natural Working Fluids at Purdue*, pp. 323–330.

Thorin, E., 2000, *Power cycles with ammonia-water mixtures as working fluid*, Doctoral Thesis, KTH, ISRN KTH/KET/R-119-SE

Yan, J., 1991, *On thermodynamic cycles with Non-Azeotropic mixtures as working fluids*, Doctoral Thesis, KTH, ISBN 91-7179-059-5

Zha, S.T., Y.T. Ma and X. Sun, 2003, "The development of CO_2 expander in CO_2 transcritical cycles", *Proc. of 21st IIR Internal congress of refrigeration*, ICR0089.

9 Appendix

9.1 Appendix 1— Safety Group Classifications (from IIR)

This classification consists of two alphanumeric characters (e.g. A2); the capital letter corresponds to toxicity and the digit to flammability.

9.1.1 Toxicity classification

Refrigerants are divided into two groups according to toxicity:

- Class A signifies refrigerants for which toxicity has not been identified at concentrations less than or equal to 400 ppm;
- Class B signifies refrigerants for which there is evidence of toxicity at concentrations below 400 ppm.

9.1.2 Flammability classification

Refrigerants are divided into three groups according to flammability:

- Class 1 indicates refrigerants that do not show flame propagation when tested in air at 21°C and 101 kPa;
- Class 2 indicates refrigerants having a lower flammability limit of more than 0.10 kg/m3 at 21°C and 101 kPa and a heat of combustion of less than 19 kJ/kg;

- Class 3 indicates refrigerants that are highly flammable as defined by a lower flammability limit of less than or equal to 0.10 kg/m^3 at 21°C and 101 kPa or a heat of combustion greater than or equal to 19 kJ/kg.

9.2 Appendix 2— Summary of Attached Papers

Y. Chen, P. Lundqvist, P. Platell, "Theoretical Research of Carbon Dioxide Power Cycle Application in Automobile Industry to Reduce Vehicle's Fuel Consumption", ***Applied Thermal Engineering 25 (2005)*****, pp 2041–2053**

This work discusses means to utilize low-grade energy in vehicle exhaust gases, to reduce the vehicle's fuel consumption and to make it run in a more environmentally friendly way. To utilize the energy in the exhaust gas, a CO_2 bottoming system in the vehicle's engine is proposed. Several basic cycles—according to the different design concepts—are presented, and the efficiencies are calculated using Engineering Equation Solver (EES).

Several thermodynamic models in EES show that after system optimization, in a CO_2 transcritical power cycle with a gas heater pressure of 130 bar and 200°C expansion inlet temperature, about 20% of energy in the exhaust gas can be converted into useful work. Increasing the pressure in the gas heater to 300 bar and with the same expansion inlet temperature, about 12% of the exhaust gas energy can be converted. When raising the pressure both in the gas cooler and in the gas heater, the cycle runs completely above the critical point, and the efficiency is about 19%. In addition, in the CO_2 combined cycle, the system COP is 2.32 and about 5% of exhaust gas energy can be converted.

Y. Chen, P. Lundqvist, A. Johansson, P. Platell, "A comparative study of the Carbon Dioxide Transcritical Power Cycle compared with an Organic Rankine Cycle with R123 as working fluid in Waste Heat Recovery", ***accepted for publication by Applied Thermal Engineering***

The organic rankine cycle (ORC) as a bottoming cycle to convert low-grade waste heat into useful work has been widely investigated for many years. The CO_2 transcritical power cycle, on the other hand, is scarcely treated in the available literature. A CO_2 transcritical power cycle (CO_2 TPC) shows a higher potential than an ORC when taking the behavior of the heat source and the heat transfer between heat source and working fluid in the main heat exchanger into account. This is mainly due to a better temperature glide match between heat source and working fluid. The CO_2 cycle also show no pinch limitation in the exchanger. This study looks at the performance of the CO_2 transcritical power cycle in utilizing energy from low-grade waste heat to produce useful work in comparison to an ORC using R123 as working fluid.

Due to the temperature gradients for the heat source and heat sink the thermodynamic mean temperature has been used as a reference temperature when comparing both cycles. The thermodynamic models have been developed in EES. The relative efficiencies have been calculated for both cycles. The results obtained show that when utilizing the low-grade waste heat with the same thermodynamic mean heat rejection temperature, a transcritical carbon dioxide power system gives a slightly higher power output than the organic Rankine cycle.

Y. Chen, P. Lundqvist, "Carbon dioxide cooling and power combined cycle for mobile applications", ***7th IIR Gustav Lorentzen Conference on Natural Working Fluids, Trondheim, Norway, May 28-31, 2006***

A carbon dioxide cooling and power combined system, which can provide A/C and produce power at the same time, is

proposed in this paper. The power part of the system can utilize the energy in automobile exhaust gases to produce electricity for the A/C's compressor, and thus both increases the cooling COP and decreases the vehicle's fuel consumption by reducing the compressor's energy demand. Moreover, different factors that influence the cycle's optimum working conditions are also discussed.

The software Engineering Equations Solver (EES) is used to model and to analyze the system performance. Results show that the proposed combined system can achieve a COP of 3.18 for the cooling part and 12.6% efficiency for the power part under typical working conditions. After transferring the energy gained from the cycle to its compressor, the new COP will be 4.45 and the improvement of the COP will be around 40% accordingly.

Y. Chen, "Carbon Dioxide Transcritical Power Cycle Discussion", ***Internal report in KTH, Trita REFR Report No. 05/49, ISSN 1102-0245, ISRN KTH/REFR/R-05/49-SE***

This report is a result of the PhD course in Thermodynamics at the Dept. of Energy Technology, KTH. The purpose of this report is to show general knowledge about how thermodynamic theory and thermodynamic thinking can be applied to scientific work in general and cycle analysis, etc.

The cycle being analyzed in this report is the carbon dioxide transcritical power cycle. Carbon dioxide transcritical power cycle has a good potential in utilizing the energy in low-grade heat sources. The reason for this is mainly due to the temperature glide in the supercritical region that can provide a better match to the heat source than other working fluids, thus making it possible to avoid the so-called pinching problem in the main heat exchanger that was used to obtain energy from the heat source. The fact that the carbon dioxide iso-bars in the supercritical region have a unique shape and that the temperature in the supercritical region is no longer related to

the pressure, make the carbon dioxide transcritical power cycle very different from other sub-critical power cycles. For a certain expansion inlet temperature or pressure, the means of optimizing the cycle operating conditions has a tremendous impact on cycle efficiency.

This report shows why the heat source match is important for low-grade heat source utilization. Different factors that will influence the cycle efficiencies are studied and the influences are illustrated in different figures. The reason for why the influences are bigger for lower gas heater pressures is also discussed.